KINEMATIC ANALYSIS OF HEATING, VENTILATING AND COOLING MODULE PARTS OF AUTOMOBILE AIR CONDITIONING SYSTEM USING CAE TOOLS

A thesis report submitted in partial fulfilment of the requirement for the award of

MASTER OF ENGINEERING

IN

CAD/CAM & ROBOTICS

Submitted By

BALJEET SINGH

Roll No. 800981005

Under the Guidance of

Mr. DALJEET SINGH
Assistant Professor,
Deptt. of Mech. Engg.,
TU, Patiala.

Mr. JASWINDER SINGH SAINI
Assistant Professor,
Deptt. of Mech. Engg.,
TU, Patiala.

DEPARTMENT OF MECHANICAL ENGINEERING

THAPAR UNIVERSITY

PATIALA-147004, INDIA

July-2011

DECLARATION

I hereby declare that the work in this thesis report entitled **"KINEMATIC ANALYSIS OF HEATING, VENTILATING AND COOLING MODULE PARTS OF AUTOMOBILE AIR CONDITIONING SYSTEM USING CAE TOOLS"** is an authentic record of my study carried out as a requirement for the award of degree of **Master of Engineering (CAD/CAM & Robotics)** at **Thapar University, Patiala** under the guidance of **Mr. DALJEET SINGH**, Assistant Professor, Mechanical Engineering Department, Thapar University, Patiala and **Mr. JASWINDER SINGH SAINI**, Assistant Professor, Mechanical Engineering Department, Thapar University, Patiala, during **July 2010 to June 2011.** The matter embodied in this report has not been submitted in part or full to any other university or institute for the award of any other degree.

Baljeet Singh
(Baljeet Singh)
Reg. No. 800981005

This is to certify that above declaration made by the student concerned is correct to the best of our knowledge and belief.

14/7/11
Mr. DALJEET SINGH
Assistant Professor,
Mech. Engg .Deptt.,
Thapar University,
Patiala-147004.

14-7-2011
Mr. JASWINDER SINGH SAINI
Assistant Professor,
Mech. Engg. Deptt.,
Thapar University,
Patiala-147004.

Countersigned by:

Dr. AJAY BATISH
Professor and Head,
Mech. Engg. Deptt.,
Thapar University,
Patiala-147004.

Dr. S.K. MOHAPATRA
Dean of Academic Affairs,
Thapar University,
Patiala-147004.

ACKNOWLEDGEMENT

I would like to express a deep sense of gratitude and thank profusely my guides ***Mr. Daljeet Singh*** *and* ***Mr. Jaswinder Singh Saini*** *for their sincere & invaluable guidance, suggestions and attitude, which inspired me to submit thesis report in the present form. Their dynamism and diligent enthusiasm have been highly instrumental in keeping my spirits high. Their flawless and forthright suggestions blended with an innate intelligent application have crowned my task with success.*

I am also thankful to ***Dr. Ajay Batish,*** *Professor & Head, Department of Mechanical Engineering for his encouragement and inspiration for execution of the thesis work.*

I am deeply indebted to my parents for their inspiration and ever encouraging moral support, which enabled me to pursue my studies.

I am also very thankful to the entire faculty and staff members of Mechanical Engineering Department for their intellectual support and cooperation.

Baljeet Singh

Reg. No.: 800981005

ABSTRACT

With the automotive air-conditioning industry aiming at higher levels of quality, cost effectiveness and a short time to market, the need for simulation is at an all time high. In the present work, the use of multibody dynamics approach is proposed in the simulation and analysis of the airflow control mechanisms of an automotive HVAC module for opening various doors/dampers used for passenger comfort. The movements of various parts have been kinematically analyzed. A new method for cam design has been developed which is faster and simpler than the existing method. Two HVAC kinematic mechanism are designed, one with single link configuration and other with two link configuration for the same output. The single lever configuration leads to higher torque requirement along with more space requirement. Torque required in the two link configuration is lesser than in the existing design, thus lowering the effort required to rotate the cam from the control panel.

INDEX

LIST OF FIGURES

LIST OF TABLES

ABBREVIATIONS

HVAC	Heating, Ventilating and Cooling
MBS	Multibody system
AC	Air Conditioning
CAE	Computer Aided Engineering
CAD	Computer Aided Design
FEM	Finite Element Method
FVM	Finite Volume Method
BEM	Boundary Element Method
FDM	Finite Difference Method
FEA	Finite Element Analysis
CFD	Computational Fluid Dynamics
MV	MotionView
HM	HyperMesh
COM	Centre of Mass
DAE	Differential Algebraic Equations
IGES	Initial Graphics Exchange Specification
DOF	Degrees of Freedom
SAR	Synthetic Aperture Radar
ANCF	Absolute Nodal Coordinate Formulation
HCF	Hybrid Coordinate Formulation

CHAPTER 1

INTRODUCTION

This chapter discusses the basic details and concepts of related topics associated with the present work.

1.1 METHODS TO SOLVE ANY ENGINEERING PROBLEM

Any engineering problem can be solved using the following different methods:

a) Analytical method
b) Numerical method
c) Experimental method

The following Table 1.1 shows the brief comparison of these methods:

Table 1.1: Comparison of solution methods

Analytical Method	Numerical Method	Experimental Method
Classical approach	Mathematical representation	Actual measurement
100% accurate results	Approximate, assumption made	Time consuming & needs expensive set up.
Closed form solution	Applicable even if physical prototype not available (initial design phase)	Applicable only if physical prototype is available
Complete in itself	Real life complicated problems	Results cannot be believed blindly & min. 3 to 5 prototypes must be tested

The procedure for solving a problem using the Analytical or Numerical approach is as follows:

Step1) Writing the governing equation: It represents the problem definition or in other words formulating the problem in the form of a mathematical equation.

Step2) Mathematical solution of governing equation.

Final result is summation of above two steps. In analytical approach, the results will be 100% accurate as there is no assumption at either of the two steps. But on the other hand numerical method makes approximation at both the steps and hence it is an approximate method.

Analytical methods are used for only limited number of problems because exact governing equations are available for simple problems. For complex problems governing equations with some assumptions are to be made which are then solved using numerical method.

Numerical methods like FEM are based on discretization of integral form of equation. Basic theme of all numerical methods is to make calculations at only limited number of points and then interpolate the results for the entire domain. Even before getting the solution, the variation of unknown parameters over a domain is known. For example, when meshing is carried out using linear quadrilateral elements, assumptions made is linear variation of displacement over the domain and for 8 nodded quadrilateral element, assumption is parabolic variation. This may or may not be the case in real life and hence all numerical methods are based on an initial hypothetical assumption. After getting the results there are several ways to check numerical as well as practical results, correlation, accuracy and minimization of errors.

1.2 TYPES OF NUMERICAL METHODS

Different types of numerical methods are as under:

a) **Finite Element Method (FEM):**

FEM is the most popular numerical method.

Applications – Linear, Nonlinear, buckling, Thermal, Dynamic & Fatigue analysis.

b) Boundary Element Method (BEM):

It is a very powerful and efficient technique to solve acoustics or NVH problems. Just like the finite element method it also requires nodes and elements but it considers only outer boundary of the domain. So in this case if the problem is of volume, only outer surfaces are considered. If the domain is area then only outer periphery is considered. This way it reduces dimensionality of the problem by a degree of one & thus solving it faster.

c) **Finite Volume Method (FVM):**

All computational fluid dynamics (CFD) softwares are based on FVM. Unit volume is considered in Finite Volume Method. Variable properties at nodes are pressure, velocity, area, mass etc. It is based on Navier – strokes equation.

d) **Finite Difference Method (FDM):**

Finite element and Finite difference share many common things. In general Finite difference method is described as a way to solve differential equation. It uses Taylor's series to convert differential equations to algebraic equation. It is used in combination of BEM or otherwise FVM to solve thermal and CFD coupled problems.

FEM, being the most versatile method is to be used in the present work.

1.2.1 Finite Element Method (FEM)

Finite element method is Numerical analysis technique for obtaining approximate solution to number of engineering problem. It has been applied to broad area of continuum mechanics. Because of its flexibility as an analysis tool, it has emerged as much bone to the researchers.

In number of engineering situation, it is necessary to obtain approximate solution rather than exact solution to the problem. For example to find the concentration of pollution in atmosphere, to predict the formation of tornadoes and thunderstorms are the few examples of many partial problems. The derivation of governing equation for these problems can for done without much effort, but there solution by exact method of analysis is difficult task. The difficulty in these problems lies in the fact that either the geometry or some other feature of the problem is irregular or arbitrary. In such cases approximate methods of analysis provide alternate solutions. Examples of approximation methods are finite difference method and variational method such as Rayleigh Ritz method and Galerkin method.

In Finite difference method, the model of a problem gives a point wise approximation to the governing equation. Although finite difference method is simpler but it has several disadvantage. For example we have irregular or non straight boundaries. It is difficult to apply boundary condition. The difficulty to represent geometrically complex domain is to employ non uniform and nonrectangular meshes to more a few.

FEM overcomes the difficulties of all the other methods as it provides the systematic procedure for the deviation of the approximation functions. First a geometrically complex domain is represented as a number of geometrically simple sub domains, called ‘Finite Element’. Second, the approximation functions over each finite element are derived using the idea that any continuous function can be represented by a linear combination of polynomials. In other words, FEM has the ability to formulate the solution for each Finite Elements which are then put together to report the entire problem.

1.2.2 Basic Steps in Finite Element Method

The following steps are used for analyzing a problem-

1. Pre-processing
2. Processing or Solution
3. Post processing

Preprocessing

Steps in pre-processing

a) CAD data generation / import
b) Meshing
c) Boundary conditions

There are specialized softwares for CAD, Meshing and Analysis. CAD & meshing consumes most of the time. For example- typical time for a single person to model (CAD) 4 cylinder engine block is 6 weeks & for brick meshing 7 weeks.

Boundary conditions consume least time but it is the most important step. 3 months hard work of meshing & CAD data preparation of engine block would be undone in just 1 day if boundary conditions are not applied properly.

Processing or Solution

During pre-processing user has to work hard while solution step is the turn of computer to do the job. User has to just click on the solve icon. Internally software carries out matrix formation, inversion, multiplication and solution for unknown e.g. displacement and then find strain & stress for analysis.

Software uses the equation, $[\boldsymbol{F}] = [\boldsymbol{K}]\,[\boldsymbol{\delta}]$

Where,

$[F]$ = Force matrix.

$[\delta]$ = Displacement matrix.

$[K]$ = Stiffness matrix, the characteristic property of element depends on geometry as well as material.

Steps in Processing

a) Compute the element stiffness matrix

After the continuum is discretized with the discrete element shapes and the number, then the element stiffness matrix is formulated. Basically it is matrix formed by using the governing equations which tells how a parameter varies in the matrix. It is a square matrix with its size depending upon the degree of freedom of each node i.e. *[No. of columns] = [No. of rows] = No. of nodes in an element* × *Degree of freedom.*

There are 3 methods for deriving Stiffness Matrix:

1) Direct method – Easy to understand but difficult to program. It is not used for commercial software code generation.
2) Variational method – Rayleigh – Ritz method: difficult to understand, moderate from code writing point of view.
3) Weighted Residual method – Galerkin method: difficult to understand but easy from programming point of view. This method is used in most of the commercial softwares.

b) Compute the overall stiffness matrix

Previous step we have found the algebraic equation that give the characteristic of the element now all those algebraic equation are combined together to form a complete set of equation that govern the domain or structure. All the element stiffness matrices generated in last step are combined to form a overall stiffness matrix. It is a square matrix with size as *[No. of columns] = [No. of rows] = Total No. of nodes in the body* × *Degree of freedom.* It is always a symmetric matrix.

c) Formation of Element load matrix

Load applied on the body is very important parameter in any problem load applied inside the element is transferred at the node and an element load matrix is formed, it is a column matrix with *[No. of rows] = No. of nodes in an element × Degree of freedom.*

d) Formation of the overall load matrix

Like the overall stiffness matrix the element load matrix is assembled to form the overall load matrix. It is a column matrix with *[No. of rows] = Total No. of nodes in the body × Degree of the freedom).*

Post Processing

Post processing is viewing results, verifications, conclusions and thinking about what steps could be taken to improve the design

1.2.3 Applications of Finite Element Method

The various types of analysis, which can be done with FEM are -:

1) Linear static analysis
2) Dynamic analysis
3) Buckling analysis
4) Thermal analysis
5) Fatigue analysis
6) Optimization
7) CFD analysis
8) Crash analysis

Linear Static Analysis

It is the simplest and most commonly used type of analysis. Linear means straight line. $\boldsymbol{\sigma} = \boldsymbol{\varepsilon}\, \boldsymbol{E}$ is an equation of straight line ($y = m\,x$) passing through origin. "$\boldsymbol{E}$" Elastic Modulus is slope of the curve and is a constant. In real life after crossing yield point material follows non linear curve but software follows same straight line.

There are two conditions for static analysis:

a) No variation of force with respect to time (dead weight), $dF/dt = 0$
b) Equilibrium condition, $\sum Force = 0, \sum Moments = 0$

Practical applications: All Aerospace, Automobile, Offshore and civil engineering industries perform linear static analysis.

Commonly used softwares: Nastran, Ansys, Abaqus, I-deas, Radioss, Cosmos, UG, Pro Mechanica, Catia etc.

Dynamic Analysis

Static analysis does not take in to account variation of load with respect to time. Output in the form of stress, displacement etc. with respect to time could be predicted by dynamic analysis.

Practical applications: Dynamic behaviour of components subjected to dynamic loads.

Commonly used software: Nastran, Ansys, Abaqus, Matlab, I-deas NX, Radioss etc.

Linear Buckling Analysis

Linear buckling analysis is applicable for only compressive load. It is used to analyze the slender beams and sheet metal parts. Output of analysis is Critical value of load.

Practical applications: Commonly used for civil engineering applications. Mechanical engineering applications- vacuum vessel, long gear shifted rod analysis etc.

Commonly used softwares: Nastran, Anys, Abaqus etc.

Thermal Analysis

Thermal analysis is used to predict the thermal response of structures. Adequate knowledge of temperature distribution in structures, thermal flux and structural response to thermal gradients is critical to successful designs.

Practical applications: Engine, radiator, exhaust system, heat exchanger, power plants, satellite design etc.

Commonly used softwares: Ansys, Nastran, Abaqus, I-deas NX etc.

Fatigue Analysis

Fatigue analysis is used to calculate the life of the structure when subjected to repetitive load. S-N curve (alternating stress vs. cycles) or ε-N (alternating strain vs. reversals) is the base for fatigue calculation (like σ-ε diagram for static analysis).

Practical applications: Applicable to all components subjected to dynamic loading i.e. all automobile components. Fatigue accounts for 90% of failure in the real life.

Commonly used softwares: MSC Fatigue, FEMFAT, FE SAFE, LMS etc.

Optimization

Optimization analysis is used to optimize the geometric parameters and shapes of over or under designed components.

Optimization for geometry parameters, work well at individual component level rather than complicated assemblies. Software is not useful to add or remove the geometry but it works only within specific limits.

Shape optimization is usually restricted to linear static or normal mode of dynamics. It is good tool for innovation kind of product (when initial shape is not known or fixed) Software can help for addition or removal of geometry.

Practical applications: Applicable to any component which is over or under designed.

Commonly used Software: OptiSstruct, Tosca,Nastran, Ansys etc.

CFD Analysis

CFD is the branch of the fluid mechanics which use the numerical method to analyse the fluid dynamic problems. It is based on the Navier- Stroke equations (Mass, Momentum and Energy conservation equilibrium equations).

Practical application: Drag prediction and stream lining of a car, combustion chamber design to check an optimum fuel – air mixing, Aeroplane design etc.

*Commonly used Softwar*e: Fluent,Star CD, CFX, CFDExpert etc.

Crash Analysis

Crash analysis is performed to find deformation, stress and energy absorbing capacity of various structural components of a vehicle hitting a stationary or moving object. Crash analysis can also be done to find the effects of crash on human body and making the ride safe for driver as well as passengers.

Commonly used softwares: LS-Dyna, Pamcarsh, Radioss, Abaqus-Explicit, Madymo etc.

1.3 MULTIBODY SYSTEM

A MultiBody System (MBS) can be defined as a collection of bodies acted upon by forces of different origins and interconnected to each other by different types of joints that constraint their motion. The forces applied to the system components may include those resulting from contact- impact, gravity, joint constraints, friction, external applications and the interaction with other systems such as fluids, tires or wheel-rail contact. Types of kinematic constraints include various types of joints eg:

a) Revolute joints
b) Translational joints
c) Spherical joints
d) Cylindrical joints

The kinematic constraints may also be in the form of prescribed trajectories for given points of the system components. The mechanical systems included under the definition of MBS comprise robots, heavy machinery, automobile suspension and steering systems, machinery tools, animal bodies. However, the range of systems that can be represented by MBS models is expanding and new exciting applications are being proposed every day.

Fig.1.1 shows a typical multibody system. It is usually denoted as slider-crank mechanism. The mechanism is used to transform rotational motion into translational motion by means of a rotating driving beam, a connection rod and a sliding body. In the given system, a flexible body is used for the connection rod. The sliding mass is not allowed to rotate and three revolute joints are used to connect the bodies. While each body has six degrees of freedom in space, the kinematical conditions lead to one degree of freedom for the whole system.

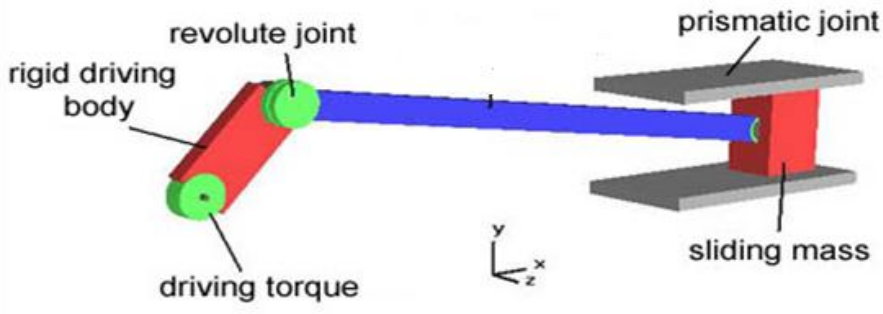

Figure 1.1: MultiBody System

1.3.1 Kinematic and Dynamic Analysis of Multibody Systems

In dealing with the study of multibody system motion, two different types of analysis can be performed, Kinematics analysis and Dynamic analysis. The Kinematic analysis consists in the study of the system’s motion independently of the forces that produce it, involving the determination of position, velocity and acceleration of the systems components. In Kinematic analysis, only the interaction between the geometry and the motions of the system is analyzed and obtained. Since the interaction between the forces and the system's motion is not considered, the motion of the system needs to be specified to some extent, i.e. the Kinematic characteristics of some driving elements need to be prescribed, while the kinematic motion characteristics of the remaining elements are obtained using the Kinematic constraint equations, which describe the topology of the system.

The Dynamic analysis of multibody systems aims at understanding the relationship between the motions of the system parts and causation of the motion, including external applied forces and moments. The motion of the system is, in general, not prescribed, its calculation being one of the principal objectives of the analysis. The dynamic analysis also provides a way to estimate external forces that depend on the relative position between the system components, such as the forces exerted by springs, dampers and actuators. Furthermore it is also possible to estimate the external forces that are developed as a consequence of the interaction between the system components and the surrounding environment, such as contact-impact and friction forces. The internal reaction forces and moments generated at the kinematic joints are also obtained in the dynamic analysis. These reaction forces and moments prevent the occurrence of the relative motions, in prescribed directions, between the bodies connected via kinematic joints.

1.3.2 Degrees of Freedom

The Degrees of Freedom (DOF) denote the number of independent kinematical possibilities to move. A rigid body has six degrees of freedom in the case of general spatial motion, three translational and three rotational. In the case of planar motion, a body has only three degrees of freedom, one rotational and two translational.

The DOF, n of a plane mechanism is calculated using Kutzbach Criterion [11].

$$n = 3\,(l-1) - 2j - h$$

Where,

l = number of links.

j = number of lower pairs.

h = number of higher pairs.

For 3D mechanism

$$n = 6 \times number\ of\ active\ elements - number\ of\ constraints$$

1.3.3 Constraints

Constraints are the restrictions placed on a part's movement in specific degree of freedom. Different types of joints constrain the relative movement of kinematic links. Different types of joints are shown in Fig. 1.2

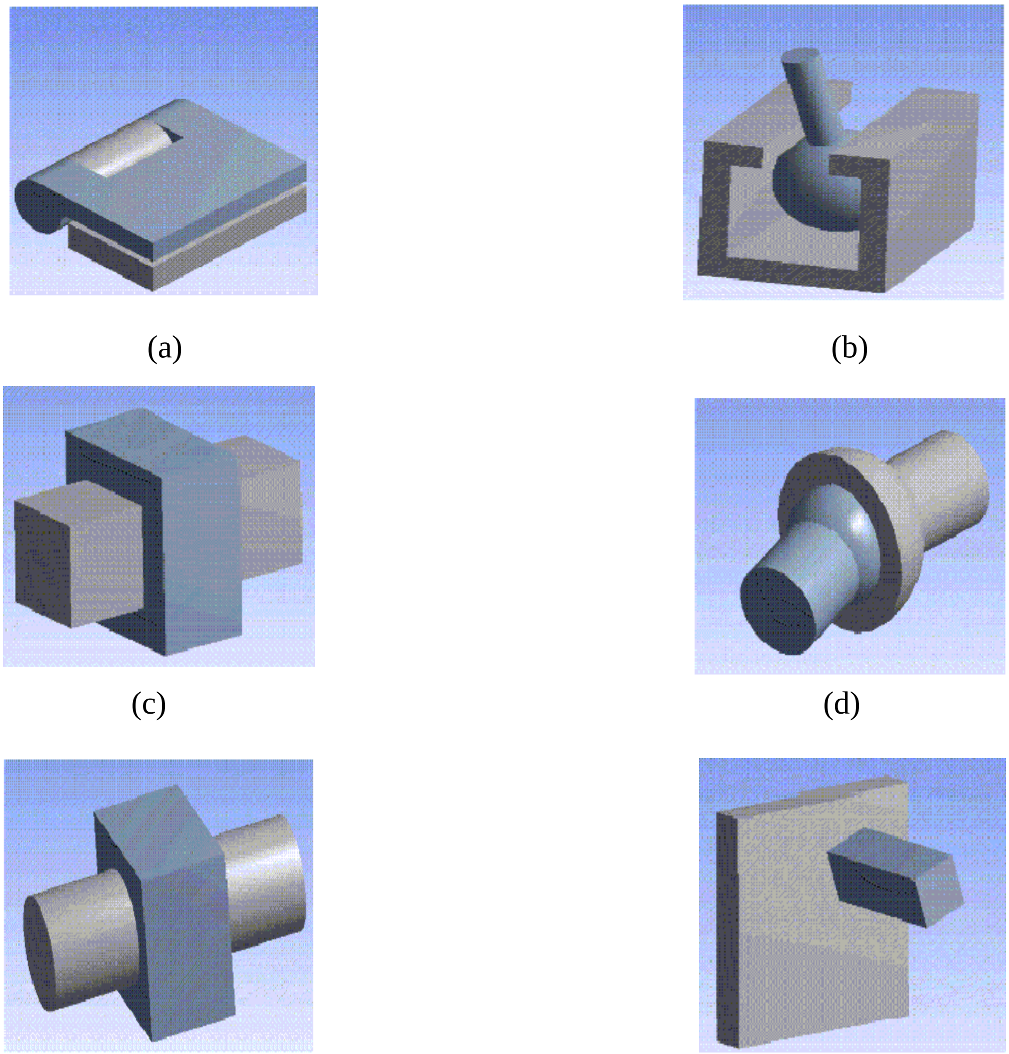

(a) (b) (c) (d) (e) (f)

Figure 1.2: Types of Joints

(a) Revolute Joint (*n* = 1); (b) Slot Joint (*n* = 4); (c) Translation Joint (*n* = 1); (d) Spherical Joint (*n* = 3); (e) Cylindrical Joint (*n* = 2); (f) Planar Joint (*n* = 3)

1.3.4 Dependent and Independent Coordinates

In order to describe a multibody system, the first important point to consider is that of choosing a mathematical model that can describe its position and motion. In other words, select a set of parameters or coordinates that will unequivocally define the position, velocity, and acceleration of the multibody system at all times.

There are two systems of coordinates:

a) Independent coordinate system
b) Dependent coordinate system

In independent coordinate system, the number of coordinates required to model the motion of system is equal to the number of degrees of freedom of motion of the multibody system and is thereby minimal. In dependent coordinate system the number of coordinates required is larger than that of the degrees of freedom, which can describe the multibody system much more easily but which are not independent, but interrelated through certain equations known as constraint equations. The number of constraints is equal to the difference between the number of dependent coordinates and the number of degrees of freedom. Constraint equations are generally nonlinear, and play a main role in the kinematics and dynamics of multibody systems.

Independent coordinates directly determine the position of the input bodies or the value of the externally driven coordinates, but not the position of the entire system. For some particular applications, independent coordinates can be very useful to describe with a minimum data set the actual velocities or accelerations and small variations in the position. In addition, they may lead to the highest computational efficiency. For general cases, dependent coordinate system is used, which uniquely determine the position of all the bodies.

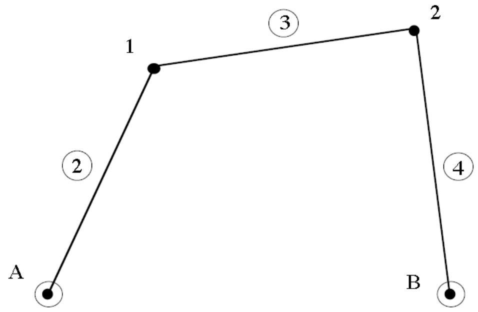

Figure 1.3: Four bar mechanism

Fig.1.3 shows a four-bar mechanism modeled with Cartesian coordinates of points 1 and 2. There are four dependent coordinates (x_1, y_1, x_2, y_2) and the mechanism has one degree of freedom. Hence, there should be three constraint equations relating the four dependent coordinates. The constraint equations shall guarantee that points 1 and 2 move in accordance with the limitations imposed on them by the three moving bars of the four-bar mechanism. It is precisely from there that the three constraint equations arise: from the fact of imposing the rigid body condition (a constant distance between points) on the three elements of the mechanism. These conditions can be formulated mathematically as follows:

$$(x_1 - x_A)^2 + (y_1 - y_A)^2 - l_2{}^2 = 0$$

$$(x_2 - x_1)^2 + (y_2 - y_1)^2 - l_3{}^2 = 0$$

$$(x_2 - x_B)^2 + (y_2 - y_B)^2 - l_4{}^2 = 0$$

These are the three constraint non linear equations that correspond to the mechanism shown. A similar system of equations can be established for any other type of coordinates and for any other multibody system.

Two types of Dependent coordinate systems which can be used are:

a) Absolute dependent coordinate system - absolute coordinates define the position of each element in relation to a fixed reference frame.
b) Relative dependent coordinate system - relative coordinates define the position of each element in relation to the previous element in the kinematic chain

1.3.5 Equation of Motion for Multibody System

A multibody system is defined as consisting of a set of interconnected rigid bodies that undergo large displacements and rotations. Tracking the motion of body, *i* in a global coordinate system, $(x_i' - y_i')$ is achieved by fixing a reference frame, $(x_{\mathrm{i}} - y_{\mathrm{i}})$ on each body. Body, *i* in the system can then be located by specifying the origin of the corresponding body-fixed coordinates expressed as

$$\mathrm{q}_i = [x, y, \phi]_i^T \tag{1.1}$$

In Eq. (1.1), ϕ denotes the relative angle between the body's reference frame and the global coordinate system (i.e., orientation). Thus, for a multibody system a set of generalized coordinates, as shown in Eq. (1.2), uniquely define the position and orientation of all bodies in the system.

$$q = [[x, y, \phi]_1^T, [x, y, \phi]_2^T, \ldots\ldots, [x, y, \phi]_i^T]^T \tag{1.2}$$

The bodies in a multibody system are interconnected by joints which impose conditions on their relative motion. Consequently, the generalized coordinates are usually not independent. When these conditions are expressed as algebraic equations in terms of the generalized coordinates and time,t they are referred to as holonomic kinematic constraints and are expressed as:

$$\phi\ (q, t)\ =\ 0 \tag{1.3}$$

Assuming that the multibody system of interest is properly constrained and the number of constraints equals the generalized coordinates, Eq. (1.3) can simultaneously be solved to uniquely determine the position, q of the system components at any time. Furthermore, the velocities and acceleration of all components can be determined using Eq. (1.4) and (1.5).

$$\phi_q \dot{q} = -\ \phi_t\ , \tag{1.4}$$

$$\phi_q \ddot{q} = -\left(\phi_q \dot{q}\ \right)_q -\ 2\phi_{qt} \dot{q}\ -\ \phi_{tt} = \Upsilon \tag{1.5}$$

The Eqs. (1.4) and (1.5) are obtained by differentiating Eq. (1.3) with respect to time. The solution of the constraint, velocity and acceleration, equations to determine the motion of the system is referred to as kinematic analysis. In order to determine the system response due to externally applied loads, it is necessary to perform a dynamic analysis, which requires the assembly and solution of the differential algebraic equations of motion. The equation can be expressed as:

$$M\ddot{q} + \phi_q^T \lambda = Q^A \tag{1.6}$$

Where, M is the mass matrix consisting of masses and moments of inertia for the system components, $\ddot{q}$ and ϕ_q^T are the acceleration vector and Jacobian of the constraints, respectively, λ is a vector of Lagrange multipliers, and Q^A is a vector of externally applied loads. In the present work the body-fixed coordinate system at the Centre of Mass (COM) of the corresponding body. This significantly simplifies the general form of the equations of motion. The product of the Jacobian and the vector of Lagrange multipliers is in fact the vector of reaction forces. For an unconstrained system, the vector of Lagrange multipliers is zero, so the Eq. (1.6) reduces to

$$M\ddot{q} = Q^A \tag{1.7}$$

Eqs. (1.5) and (1.6) can be combined to form a mixed system of Differential Algebraic Equations (DAE) of motion. The equations are expressed as:

$$\begin{bmatrix} M & \phi_q^T \\ \phi_q & 0 \end{bmatrix} \begin{bmatrix} \ddot{q} \\ \lambda \end{bmatrix} = \begin{bmatrix} Q^A \\ \Upsilon \end{bmatrix} \tag{1.8}$$

Where, $\phi_q\ddot{q} = -\left(\phi_q\dot{q}\right)_q - 2\phi_{qt}\dot{q} - \phi_{tt} = \Upsilon$. The solution procedure for this Eq. (1.8), which determines the dynamics of a system, is summarized in the form of a flow chart shown in Fig. 1.4.

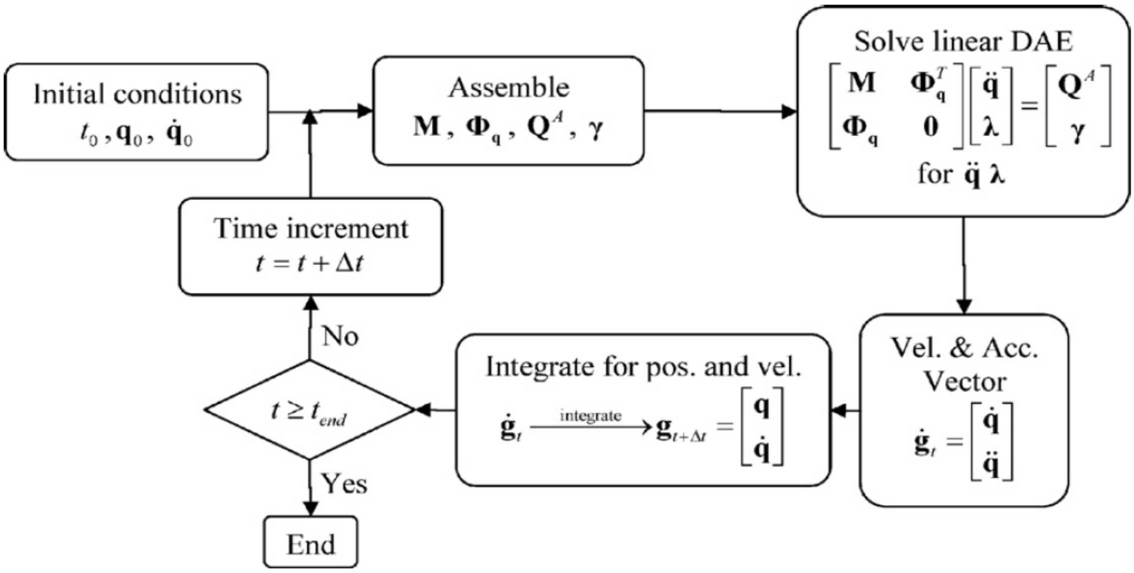

Figure 1.4: Integration procedure for the Differential Algebraic Equation

CHAPTER 2

LITERATURE REVIEW

The following section presents the review of the work done in kinematic and dynamic analysis of vehicles.

2.1 LITERATURE REVIEW

Alias and Majid [1] performed Multibody dynamic analysis and topology optimization of Wiper Mechanism using Motionview / Motionsolve. A methodology was introduced to simulate the whole contact range of the wiper blade to be constantly in contact with the windshield glass for multibody dynamic analysis by using Altair MotionView / MotionSolve and finally topology optimization using Altair OptiStruct. A kinematic wiper system was modelled using Altair MotionView with the application of joints and introduced contact between the wiper blade and the windscreen glass with contact components of both flexible and rigid. The maximum stress and forces were measured during the wipping process. Then the methodology of topology optimization was introduced to analyze the best possible shape of the wiper bracket that has strength and durability but yet cost effective. Multibody analysis reduced 22% mass from original design and also reduced the complexity of the casting. To verify the optimized wiper bracket design, MBD analysis was re-conducted in Altair MotionSolve based on the previous boundary conditions. As a result, an overall maximum stress was determined to be below the material yield stress, even though some small increment of stress values were detected as compared to original design. The result validated the stress level for the optimized wiper bracket.

Bertorelli *et al.* [2] performed structural crash analysis with ADAMS to make comparison between multibody and FEM approaches. The work dealt with modelling of mechanical structures subjected to impact loading with a multibody approach. Main goal was to verify and evaluate the capabilities of the commercial rigid-body code ADAMS in order to analyze the deep plastic collapse behaviour of structural members. A "basic element" being able to describe the bending behaviour of plastic hinges was developed. The model was validated by comparison with an analytical solution of a simple non-linear model solving the ordinary differential equation of motion of the system subjected to impulse load and the two solutions have been compared. It was concluded from the study that ADAMS could be used successfully to study structural impact problems that involve large displacements and highly non-linear material behaviour. Global approach with ADAMS allowed the designer to obtain a good first-stage solution in a very short time, with a good confidence of results.

Bauchau and Ju [3] modelled the friction phenomena in flexible multibody dynamics and proposed an approach to increase the versatility and accuracy of unilateral contact models in multibody systems. Two joint configurations were developed, the planar and spatial clearance joints that can deal with typical configurations where contact and clearance were likely to occur. More general configurations could be developed based on the same principles. The kinematic analysis of the joint yielded two important quantities: the relative distance between the bodies that drives the intermittent contact model and the relative tangential velocity that drives the friction model. An arbitrary contact force–approach relationship was used for the contact model. For the friction model, the use of the LuGre model [5] was proposed in the work. This physics based model was capable of capturing a number of experimentally observed phenomena associated with friction. From a numerical stand point, it eliminated the discontinuity associated with Coulomb's friction law. Discretizations were proposed for both normal contact and friction forces that implied an energy balance for the former and energy dissipation for the latter. When combined with the energy decaying schemes used in the effort, these properties of the discretization guaranteed the nonlinear stability of the overall numerical process. The numerical simulations relied on time step adaptivity; simple, yet effective strategies were given to evaluate the required time step size when contact and friction were occurring. The efficiency of the proposed approach was demonstrated by realistic numerical examples that demonstrate the coupling between contact and friction forces and the overall dynamic response of the system.

Espadafor *et al.* [6] analysed a catastrophic crankshaft failure of a four stroke 18 V diesel engine of a power plant for electrical generation when running at a nominal speed of 1500 rpm. The rated power of the engine was 1.5 MW, and before failure it had accumulated 20,000 hrs in service operating mainly at full load. The fracture occurred in the web between the 2nd journal and the 2nd crankpin. The mechanical properties of the crankshaft including tensile properties and surface hardness were evaluated. Fractographic studies showed that fatigue was the dominant mechanism of crankshaft failure, where the beach marks can be clearly identified. A thin and very hard zone was discovered in the template surface close to the fracture initiation point, which suggested that it was the origin of the fatigue fracture. A finite element model of the crankshaft predicted that the most heavily loaded areas match the fractured zone. The simulation model was composed of a dynamic lumped model linked to a finite element model. The analysis of the simulation results revealed different zones where the maximum stresses were reached, which could be considered to have the same failure probability, with the estimated stress level for fatigue initiation being in the range $260-275\ MPa$. One of these zones coincided with the zone where the fatigue failure originated and so it was well matched to the results of the material analyses. It was concluded that the failure was produced in one of the most stressed areas, where the material had anomalies

Flores and Ambrosio [7] studied the revolute joints with clearance in multibody systems. Clearances always exist in real joints in order to ensure the correct relative motion between the connected bodies being the gap associated to them a result of machining tolerance, wear, and local deformations. Clearance at different joints is the source for impact forces, resulting in wear and tear of the joints, and consequently the degradation of the system performance. The model for planar revolute joints was based on a thorough geometric description of contact conditions and on a continuous contact force model, which represented the impact forces. The model proposed lead to realistic contact forces. These forces correlated well with the joint reaction forces of an ideal revolute joint, which correspond to a null joint clearance.

The basic ingredients of the model proposed were the contact detection strategy and the contact force models used. The proposed procedures were demonstrated through the dynamical analysis of a slider-crank mechanism that has a revolute joint with clearance. It was observed that the energy dissipation of the continuous contact model proposed by Lankarani and Nikravesh [12] results in long periods of time when the journal seats in the bearing, thus leading to a much smoother dynamic response of the system.

Flores [8] performed Modeling and simulation of wear in revolute clearance joints in multibody systems. A general methodology for modeling and evaluating wear in mechanical systems was presented in the work. An approach was developed under the framework of a multibody systems formulation. The wear model used was based on the generalized Archard’s equation, which relates the volume of material loss with physical and geometrical properties of the contacting bodies. The wear approach was quite easy and straightforward to implement in a computational program. An elementary four bar mechanism, which includes a revolute joint with clearance, was used as a numerical example application, to show the wear phenomenon and its global dynamics behavior. From the main qualitative and quantitative results obtained, it was demonstrated that the wear depth along the joint surface is non-uniform, due to the fact that the contact between the journal and bearing walls is wider and more frequent is some specific regions.

Greco and Coda [9] proposed Positional FEM formulation for flexible multi-body dynamic analysis. A new, simple and accurate formulation to solve dynamic geometrical nonlinear problems with large deflections applied to multi-body analysis was proposed. The formulation was based on position description, simplifying the understanding and the implementation of large deflection analysis when compared with typical FEM formulations. The Newmark time integrator scheme was successfully applied to integrate positions along time. An explanatory section regarding the way followed to consider free joints for multi-body plane analysis was given. Four examples were shown demonstrating the accuracy and possibilities of the formulation, mainly for multibody applications. The influences of different mass matrix approaches were also provided, showing that the overall structural behaviour was slightly affected by mass considerations when slender bars were considered.

He et *al.* [10] studied failure analysis of an automobile damper spring tower and investigated the cause of a passenger car's damper spring tower early failure. Inspection of the road surface, tire inflation pressure, suspension, and service load were firstly done in order to determine the further test procedures and analysis methods. The static stress of the spring tower caused by the body weight was calculated by finite element model. Public road tests with an equipped car were carried out to simulate the real usage by the customers. With the measured strain signals of different test conditions and local strain–life method, fatigue life prediction was made. The calculated fatigue life coincided with the actual failure mileage, and it turned out that the broken spring damper caused the early failure of the spring tower. It was suggested that more emphasis should be taken on the durability design and test of the spring damper. Fatigue calculation results showed good coincidence with the actual failure mileage of the spring tower. It turned out the failure was caused by the failure of the spring damper. The spring damper's manufacture quality or design parameters and elevated inflation pressure, bad road surface, heavy load of the car caused the spring damper to be over compressed and thus led to the elastomer's failure and oil leakage.

Mukras *et al.* [13] analysed planar multibody systems with revolute joint wear and described a procedure to analyze planar multibody systems experiencing wear at the revolute joint. The procedure incorporated the effects of non-ideal revolute joint and included joint clearance. Unlike the ideal joint which uses kinematic constraints to restrict the motion of the joint components, the non-ideal joint uses force constraints to guide the motion of the joint components. The procedure assumed that the joint components can exhibit one of three configurations: (1) free-flight; (2) impact; and (3) following motion. In the case of the free-flight, no contact occurred between the components. This situation was modelled by requiring zero contact/reaction force so that no restriction was imposed on the motion of the joint components. For the impact and following motion, contact between the joint components was established. Contact force was developed based on the amount of penetration experienced during contact. By applying the contact force on the opposing joint components, the force constraints were enforced. Wear was then incorporated by allowing the contact surfaces of the joint components to evolve while iteratively performing the dynamic analysis. The evolution was dictated by an iterative wear prediction procedure which estimates wear based on the joint reaction force and the relative sliding distance between the joint components.

Magheri *et al.* [14] developed an innovative wheel–rail contact model for multibody applications. The model considered the wheel and the rail as elastic deformable bodies and required numerical solution of Navier's elasticity equation. The contact between wheel and rail was described by means of suitable analytical contact conditions. The contact model was subsequently inserted into a multibody model of a benchmark railway vehicle (the Manchester Wagon) in order to obtain a complete model of the wagon. The complete model was implemented in the Matlab/Simulink environment. Numerical simulations of the vehicle dynamics were carried out on many different railway tracks with the aim of evaluating the performance of the model. The main objective was to achieve a better integration between the differential and multi- body modelling. This kind of integration was almost absent in the literature (especially in the railway field) due to the computational cost and to the memory consumption. It was, however, very important as only differential modelling allows accurate analysis of the contact problem (in terms of contact forces, position and shape of the contact patch, stresses and strains), while multibody modelling were generally accepted as the current standard for studying railway dynamics. The study concluded that the performance of the Matlab model turned out to be good both in terms of output accuracy (kinematic variables, contact forces and contact patch) and in terms of numerical efficiency (performance of the numerical algorithms and time consumption), thus satisfying the main objectives of the study.

Neto *et al.* [15] proposed a multibody based methodology for the analysis of flexible systems made of composite materials. The flexible multibody dynamics formulations of complex models were extended to include elastic components made of laminated composite materials. The only limitation for the deformation of a structural member was that it must be elastic and linear when described in a body fixed frame. A finite element model for each flexible body was obtained such that the nodal coordinates were described with respect to the body fixed frame and the inertia terms involved in the mass matrix and gyroscopic force vector used a diagonalized mass description of the inertia terms. The coupling between the flexible body deformation and its rigid body motion was described using only standard finite element parameters obtained with a commercial finite element code. These elements included composite material shells and beams. For composite material beam elements, the properties of their sections were found using an asymptotic procedure proposed by Popescu B. [4]. The component mode synthesis was used to reduce the number of generalized coordinates to a reasonable dimension for complex shaped structural models of flexible bodies. The kinematic constraints between the different system components were introduced and the equations of motion of the flexible multibody system were solved using an augmented Lagrangean formulation. Finally, the methodology was applied to the analysis of the deployment of synthetic aperture radar (SAR) Antenna.

The application of the methodology was demonstrated through numerical examples consisting of synthetic aperture radar (SAR) antenna, which is an extremely flexible mechanism. First, it was shown that the use of rigid body models can hide some of the potential problems that exist in this type of systems by preventing the prediction of different types of motion. The flexible multibody model of the antenna uncovered a new configuration for the start of the unfolding motion and enabled corrective measures to be taken. The use of composite materials in the model of the antenna allowed the evaluation of the importance of different lay-ups sequences in the system response emphasizing the drawbacks of the oversimplification of the models made of isotropic materials, which, in the case of the SAR antenna unfolding, leads to the need of using a smaller moment for the actuator that started the mechanism.

Parvir *et al.* [16] performed ride and stability analysis of sports car using multibody dynamic simulation, the work summarized the joint coordinate formulation for automatic generation of the equations of motion for dynamic analysis of multibody systems. A computer program based on this formulation was used to model a sports car and simulate its dynamic response in several driving scenarios. The model contained necessary elements of the suspension system such as the leafsprings, shock absorbers, bushings, tie rods, and roll stabilizer bars. An analytical model of the pneumatic tires was incorporated in the model to determine all of the necessary interacting forces and moments between a tire and the road. The most important conclusion derived from this investigation was that the most crucial component in vehicle simulations is having a realistic tire model. Many simplifying assumptions can be made in the kinematics of a vehicle model. However, simplifying assumptions in a tire model may be justifiable for some simulations, but they may yield erroneous results in many other cases.

Schirrmacher and Bonneau [17] performed Dynamic Multibody Simulation of an Unit Injector System using ABAQUS/Explicit. An optimized combustion process is essential for an environmentally correct application of Diesel engine technology. Therefore these engines require injection systems that provide extremely high operating pressures and precisely controlled injection. The unit injector system of Bosch fulfils these requirements. The mechanics of the unit injector system was simulated using the software MSC/Adams. The integration of rigid body systems and connector elements within ABAQUS version 6 allowed for the comparison between the ABAQUS-simulation of the unit injector dynamics and the corresponding results of MSC/Adams simulation. Furthermore the pre and post processing handling was of particular interest in terms of definition of elastic and rigid bodies, definition of connectors and results animation. The ABAQUS/explicit solver was chosen due to favourable contact definitions and convergence behaviour.

It was concluded from the study that ABAQUS/Explicit was in the position to successfully simulate the UIS. In comparison to MSC/Adams the program showed following advantages:

The FEM-engineer could spare license costs if the simulation can also be performed by his FEM program, FEM-engineer was not forced to learn two different simulation programs. ABAQUS/Explicit made it possible to easily switch between rigid or elastic parts and to define rigid parts consisting of different meshes and the disadvantages were ABAQUS/Explicit couldnot handle contact between two analytical rigid surfaces, a change of the rotating speed needed several changes of other parameters (amplitude, step, time, pressure function). It was very costly, run-time errors of the user-subroutine (e.g. a negative square root) were very difficult to find and the initial arrangement of all parts was a little bit tricky.

Sugiyama *et al.* [18] developed a nonlinear elastic leaf spring model for multibody vehicle systems. The model was used in the computer simulation of multibody systems. A nonlinear finite element formulation based on the floating frame of reference approach was developed for leaf springs. It was shown that the proposed leaf spring model that accounts for the effect of windup, contact and friction between the spring leaves can be effectively used for assessing the dynamic stability of sports utility vehicles.

The study made the following three specific contributions to the literature on leaf springs: The first contribution was the development of a new nonlinear elastic formulation that can be efficiently used to model leaf springs. The formulation allowed for obtaining a reduced order model that includes all significant deformation modes. The second contribution was the development of a procedure to determine the initial pre-stressed configuration of the leaf spring, and the third contribution was the computer implementation of the proposed methods and the development of a detailed vehicle model based on the nonlinear leaf spring formulation.

Teng *et al.* [19] analysed the dynamic response of vehicle occupant in frontal crash using multibody dynamics method. The study employed the multibody dynamics method to explore frontal collision phenomena. It examined the dynamic response of the human body in a crash event and assessed the injuries sustained to the occupant's head, chest and pelvic regions. Kane's method was used to obtain the governing equations describing the response of the occupant. These equations were then coded into a computer program and solved using fourth-order Runge–Kutta methods. The multibody dynamics results were found to be in good agreement with the experimental results presented in a previous study and with the numerical results obtained from LS-DYNA3D software. The analysis costs of the multibody dynamics method were very low. Therefore, the approach can assist engineers in studying different design concepts and evaluating vehicle safety at an early stage of the research and development process.

Vadhe and Dave [20] performed Multi-Body simulation of Earthmoving Equipment using MotionView / MotionSolve. A Multibody model of excavator using Altair MotionView 8.0 was generated and then the prototype conditions were simulated using MotionSolve8.0. Multibody simulation involved the simulation of rigid body systems under the application of cylinder forces and/or motions. The link (Boom) to be designed was a considered as a flexible body. Two cycles of digging and dumping operations were simulated to determine the reaction forces generated at each joint and stresses generated on the flexible body.

It was required to simulate the complete operating cycle involving digging and dumping operations, so as to understand severe conditions for different locations of booms of an excavator. The input data available was 3D geometry of attachment, upper frame, lower frame and cabin, FE model of boom, Pressure on cylinder side and piston side of all cylinders during the cycle of operation, Stroke of all cylinders during the cycle of operation, Swing motor rotational speed during the cycle of operation. Output received was the reaction forces at each joints, severe position based on stress levels at specified strain gauge locations, Trace path of bucket tooth tip.

Using Altair MotionView and MotionSolve it was possible to simulate the complete operating cycle of hydraulic excavator

Xingguo *et al.* [21] performed Multi-body Dynamics Simulation on Flexible Crankshaft System. A virtual prototype of flexible multi-body crankshaft system of engine was used for the dynamics Simulation. The theory of flexible multi-body systems dynamics was combined with FEA method to study the crankshaft, the dynamic boundary loads on the joints in a working cycle were determined by the simulation on the crankshaft system. The real-time dynamics response of the crankshaft in a cycle was achieved. It provided an important foundation for the crankshaft optimum design. The modelling of a virtual prototype of crankshaft system, constituted by crankshaft, link, piston and so on, had three steps. First, the three-dimensional model of these parts was built in modelling software. Second, they were transferred to ADAMS, the multi-body dynamics analysis software. Finally, the kinematical pairs were simplified to the ideal constraint used in the dynamics simulation.

It was concluded that the flexible multi-body dynamics simulation was based on the crankshaft system or a virtual prototype so it can simulate mechanical behaviour of crankshaft of engine in real working condition. Comparing to the common analysis method about individual crankshaft, this method had three advantages. Firstly, the system model was more approach to the physical prototype. Secondly, it needed fewer hypotheses. Thirdly, it faced to process rather than moment, thus this method had higher analysis precision.

Yoo *et al.* [22] studied large displacement of beam with base motion using Flexible multibody simulations and experiments. Physical experiments and computer simulations, which took into account for the resistance force as a proportional damping, were performed. A shaker and function generator were used to excite the system. The experiment with a high speed camera accurately captured the large displacement of the beam. Free vibration simulation was carried out with a large damping coefficient to obtain the static equilibrium position and then, the configuration of the beam was reconstructed by using the initial position. The excitation input data of the beam in the computer simulation was obtained from the experimental results. The ANCF (absolute nodal coordinate formulation) and the HCF (hybrid coordinate formulation) which was developed by combining model coordinate formulation with the absolute nodal coordinate formulation were used in the simulations. Simulation results were compared with experimental measurements. The numerical predictions were found to be in good agreements with the experimental measurements. HCF method showed reliable results and good agreement with the results of physical experiments for large deflections of a stepped cantilever beam.

The above literature review shows that a lot of kinematic and dynamic analysis of the different components of vehicle is done. Till now very less amount of work is reported on Heating, Ventilating and Cooling (HVAC) system of the car. The present work is focused on HVAC system of the car.

CHAPTER 3

HVAC KINEMATIC MECHANISM SIMULATION

3.1 PROBLEM DEFINITION

Heating, Ventilating and Cooling (HVAC) module is a very important part of the automotive air conditioning system, shown in Fig.3.1. In order to control the air flow in various modes (foot, face, defrost) by the movement of doors / dampers, the kinematic mechanism is an integral part of any HVAC module. The design and validation of the HVAC kinematics is a crucial step in the design process of the complete module. Traditionally this design has been done with a hit and trial approach, designing the kinematic parts, making physical prototypes, testing and doing iterations, if required.

In today's era, CAD and CAE tools have made design and analysis faster and cheaper, reducing time to market, and making it possible to produce parts at lesser cost in the highly competitive automobile industry. The design of the HVAC kinematic parts using CAD tools and validation by finding the displacement of doors/dampers *w.r.t.* cam rotation and the effort required to operate the cam can be explored by using the virtual simulation CAE tools. A study of Multibody dynamics systems and the simulation techniques has been made, which is used for the proposed work.

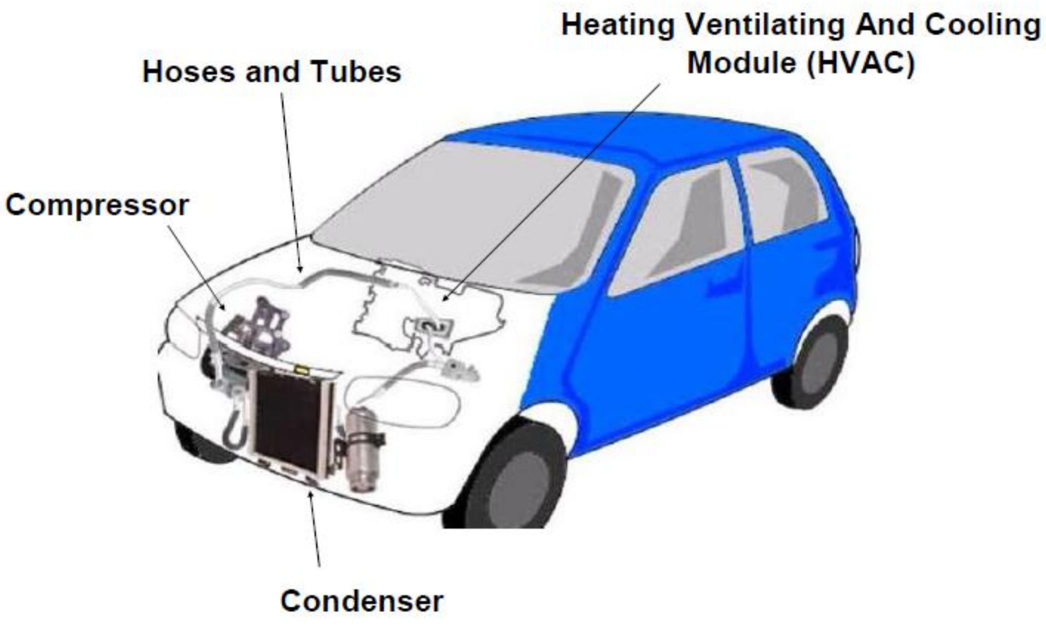

Figure 3.1: Components of car AC system

3.2 INTRODUCTION TO HVAC KINEMATIC MECHANISM

An automotive air-conditioning system has an HVAC module mounted on the firewall of the vehicle. The HVAC module consists of various parts like heater, evaporator, blower, doors/dampers, levers, cams, etc. All these parts are placed in plastic cases, and the final assembly is mounted in the vehicle. The air blown by the blower passes through the evaporator and/or the heater located inside the HVAC module and is thus cooled and/or heated up accordingly. There are openings provided in the cases for airflow in various modes. Five different modes are face, foot, bi-level (face/foot), defrost and foot/defrost. The HVAC module has a mechanism consisting of various links and a cam responsible for controlling the air flow going through these modes to the passenger cabin. The calculation of displacement and torque for these modes is a major challenge while designing the kinematics mechanism for an HVAC module. The torque required to operate the cam should not be very high, as this would lead to passenger discomfort while using the various knobs on the control panel in the vehicle. The HVAC module parts considered for the analysis are Cam, Links, Foot damper, Face damper as shown in Fig.3.2.

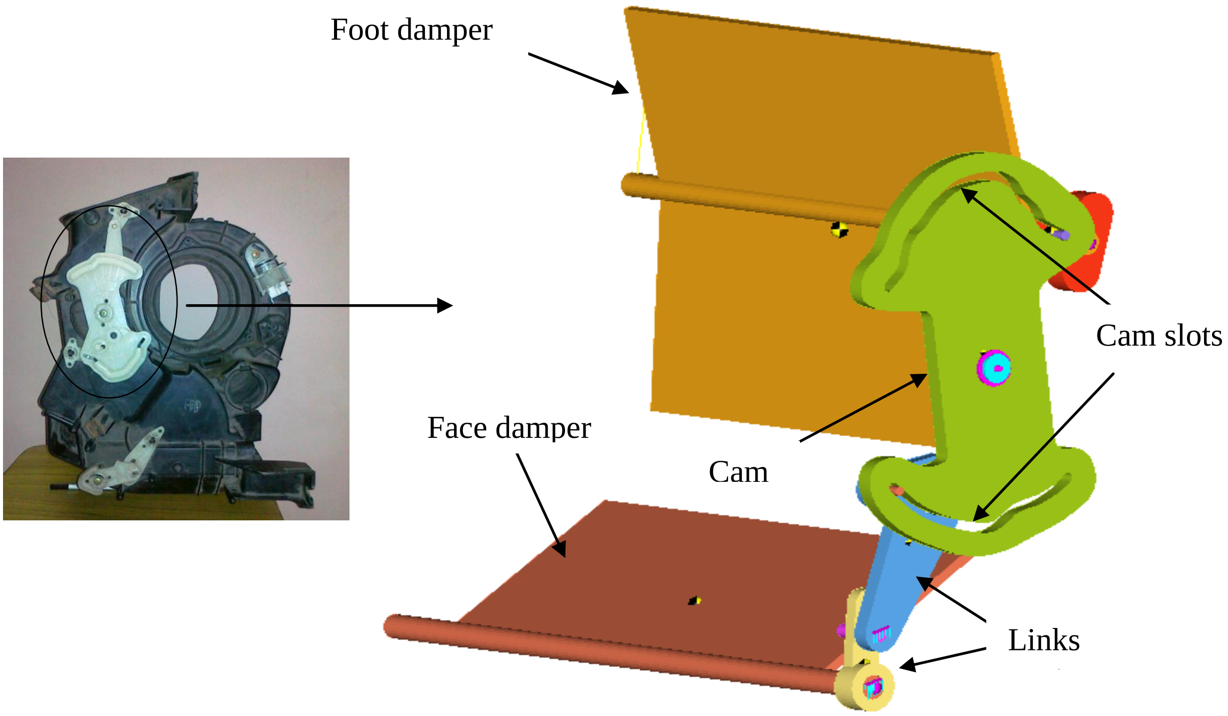

Figure 3.2: HVAC kinematic mechanism

3.3 DESIGN AND ANALYSIS CYCLE OF HVAC

The present section briefly summarizes some of the details of the background information needed for the kinematics analysis, conducted for the HVAC module using Altair HyperWorks 9.0 software.

The complete design and analysis cycle requires: (1) design of internal parts of HVAC module such as dampers, plastic cases, etc. (2) CFD analysis for damper angle design, and (3) kinematics design of HVAC mechanism. The following are the major steps for the design and analysis of the HVAC mechanism:

1. The layout design of all the internal HVAC parts is done on the basis of packaging space available in the vehicle, and the A/C system selection based on the heat load calculations.
2. Based upon this, the location, layout and design of dampers are finalized.
3. The customer data for air flow distribution and the CAD parts (HVAC cases and dampers) are given for CFD analysis, which provides the damper angles for proper air flow in various modes.
4. Based on the CFD input, the damper angles are finalized and the other parts like levers, cam, rods, etc. are designed.
5. HyperWorks is used for calculation of displacement and torque values required to operate the kinematics parts, and the results are compared with the input data for the validation of design.

The HVAC kinematic mechanism simulation (step 5) in the design and analysis cycle of HVAC is discussed in detail in the following sections.

3.4 KINEMATIC ANALYSIS OF HVAC MECHANISM

The details of the kinematics analysis done for the HVAC mechanism 'Model- A' are discussed in this section. The following steps are used to create the MV (MotionView) model, conduct the analysis and generate the results for the HVAC mechanism.

a) Reverse engineering data of HVAC components
b) CAD model of the assembly
c) Mass and inertial properties of the various parts in the mechanism
d) Discretization of the CAD geometry in HyperMesh 9.0

e) Creation of graphic H3D file for representing graphics and contacts in MV

f) Pre-processing in MV

g) Solution

h) Post processing

All the steps are described in detail below-:

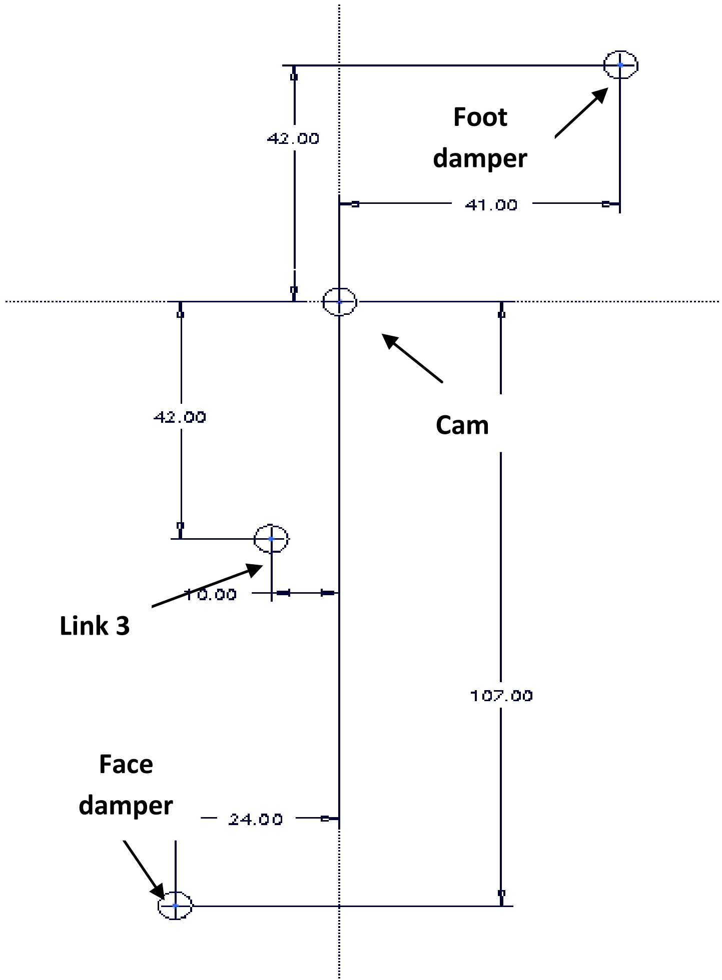

Figure 3.4: Component centre locations

3.4.1 Reverse engineering of HVAC components

The Reverse engineering of Maruti Alto HVAC unit is done with the help of different instruments. The major problem during the reverse engineering process was to measure the cam slots. Measurement was done by tracing the slots on a paper. Then number of points, about 90, were marked over the traced slot and the x and y coordinates of these points with respect to a reference frame were noted down. This coordinate data was

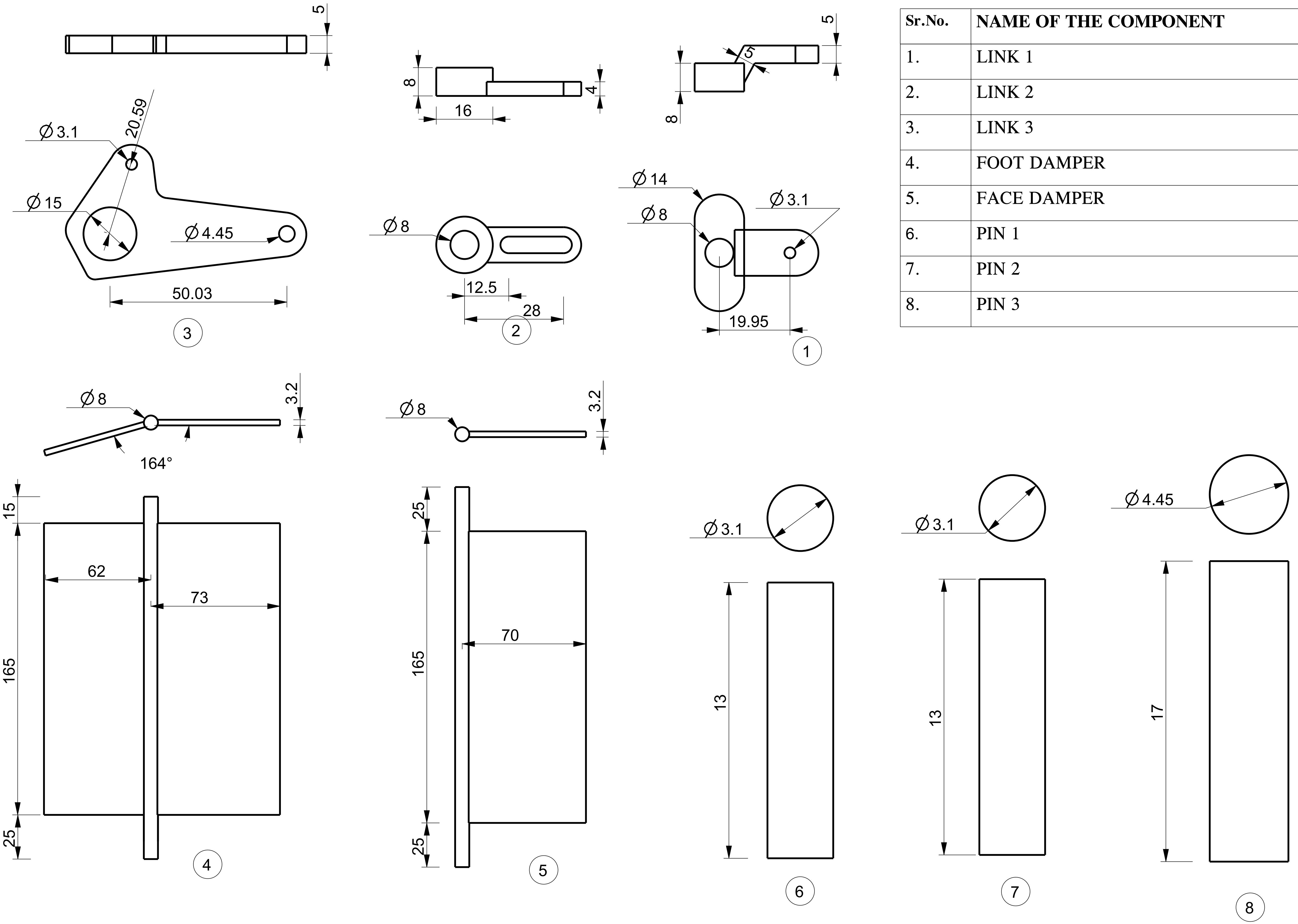

Sr.No.	NAME OF THE COMPONENT
1.	LINK 1
2.	LINK 2
3.	LINK 3
4.	FOOT DAMPER
5.	FACE DAMPER
6.	PIN 1
7.	PIN 2
8.	PIN 3

Fig.3.3 Drawings of HVAC components

entered into the CAD software and the points were joined by splines to make the slot profile. Drawings of the components are shown in Fig.3.3 and Fig.3.4 shows the component centre locations.

Fig.3.5 and 3.6 shows different points joined with the help of splines to make the slot profiles.

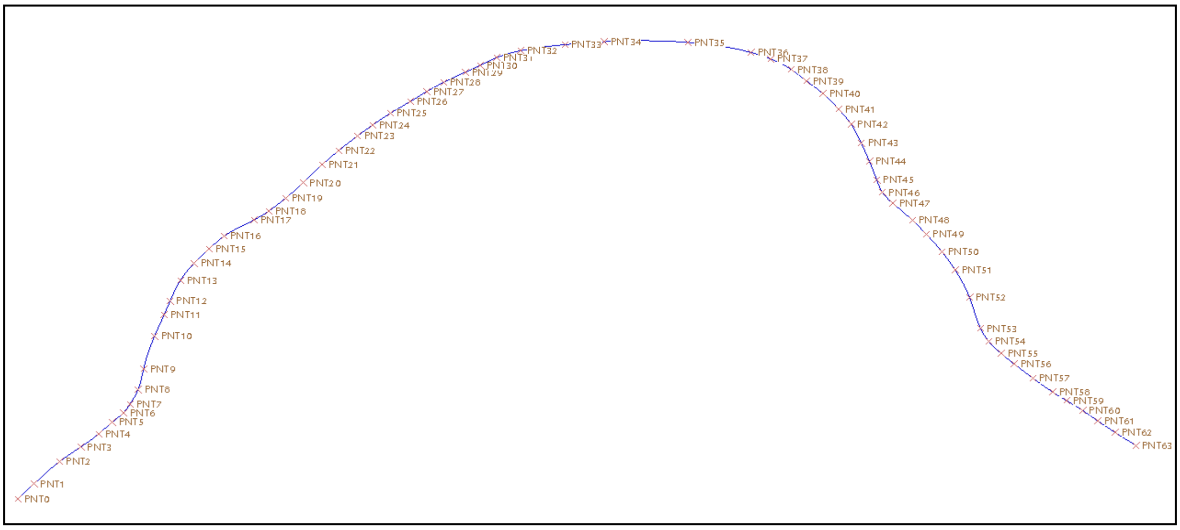

Figure 3.5: Slot 1 Profile

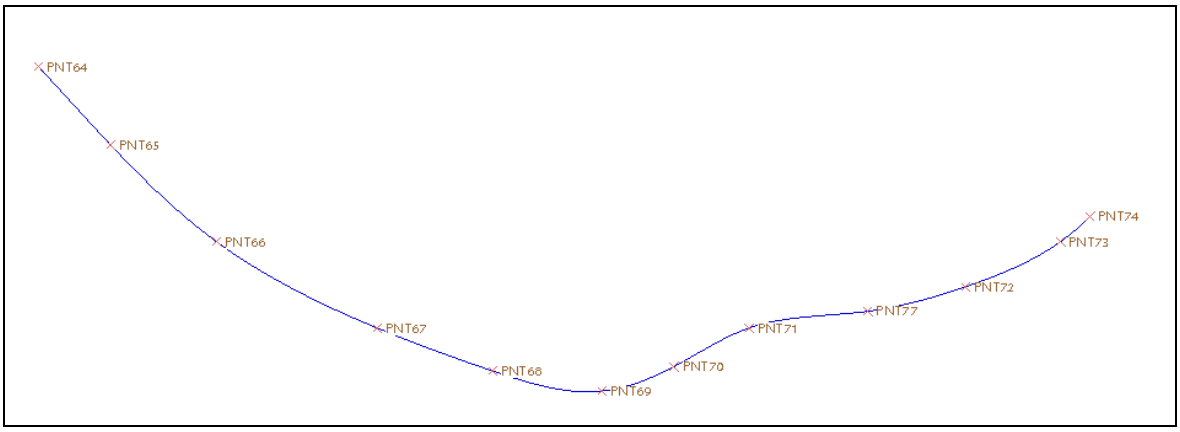

Figure 3.6: Slot 2 Profile

3.4.2 CAD modelling of HVAC components

All the components are modelled in Pro-E Wildfire 5 from the reverse engineered data. Critical work during the modelling was the exact location of all the components in the assembly, small error in the assembly may lead to large error in the kinematic movement of components. The exploded view of the assembly is shown in Fig.3.7.

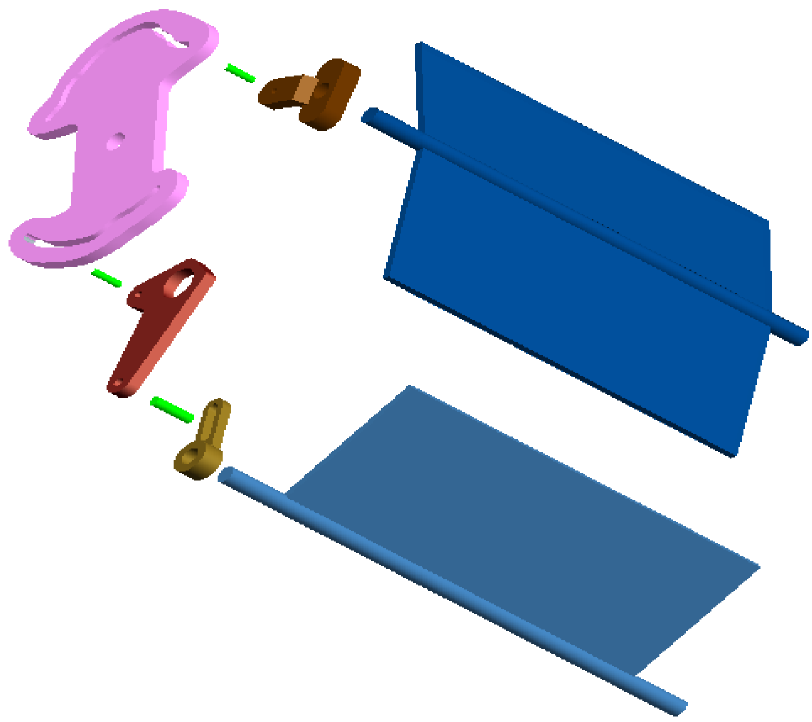

Figure 3.7: Exploded view of the assembly

3.4.3 Mass and inertia properties of HVAC components

Mass and inertia properties of all the components are needed as an input data in the multibody analysis. Steel properties are assigned to the pins and PVC (plastic) properties are assigned to the rest of components. Units are taken in $mm - kg - s$ system. The density of steel is taken $7.8270820\ \mathrm{e} - 06\ \mathrm{kg/mm^3}$ and $1.3999833\ \mathrm{e} - 06\ \mathrm{kg/mm^3}$ for PVC. Mass, Centre of gravity and inertial properties were extracted from the Pro-e assembly model of HVAC with respect to the fixed global frame.

3.4.4 Discretization of CAD geometry

The CAD parts in the assembly are imported in HyperMesh (HM) in the Initial Graphics Exchange Specification (IGES) format. The different parts are meshed in HM using triangular elements. A fine mesh is used for the contact surfaces, which are placed in a different collector/group, and the rest of the surfaces are meshed coarse. Fine meshing of cam slot and pin is shown in Fig.3.8. The direction of the normal vectors of the elements used in contacts is of particular importance. The normal vectors of the surfaces coming in contact should face each other. Fig.3.9 shows the direction of normal vectors. Element size used for meshing pins and cam slots are 0.3 mm and 1 mm for the rest of the components. Meshing is done by using different component collectors to facilitate defining contacts between pins and cam slots and to facilitate attaching graphics to the respective bodies in the MotionView.

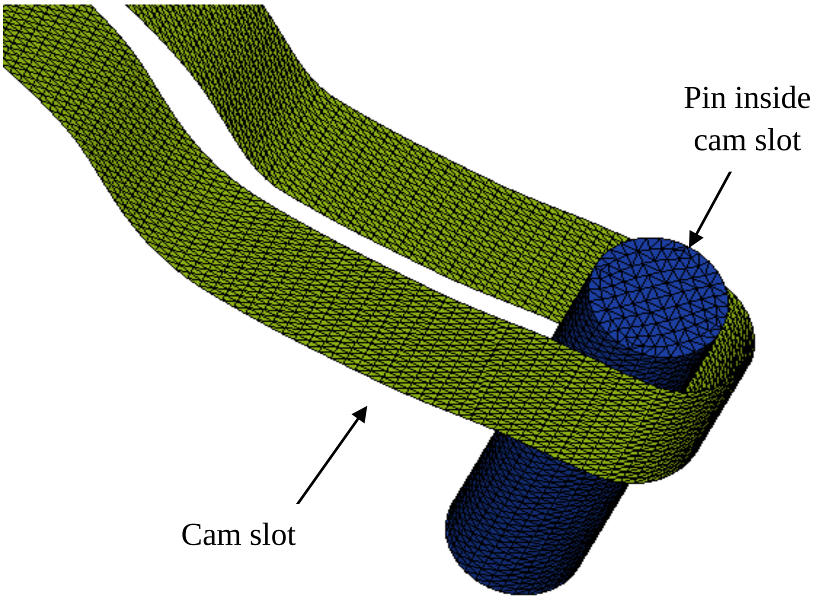

Figure 3.8: Fine meshing done to pins and cam slots

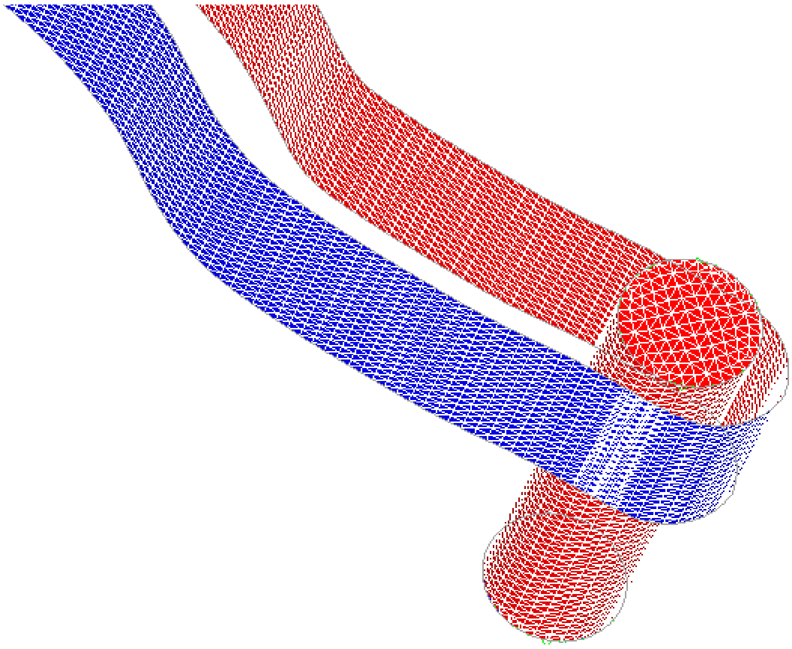

Figure 3.9: Normal vectors of contact surfaces face each other

(Red colour shows the direction of normal vectors)

3.4.5 Creation of H3D file from Mesh file

In MotionView 9.0, the tool for H3D file creation is used to make the H3D files for different parts, which are later used to attach graphics to bodies during model build up. The H3D file is created by converting the mesh file into graphics with the tool show in the Fig.3.10.

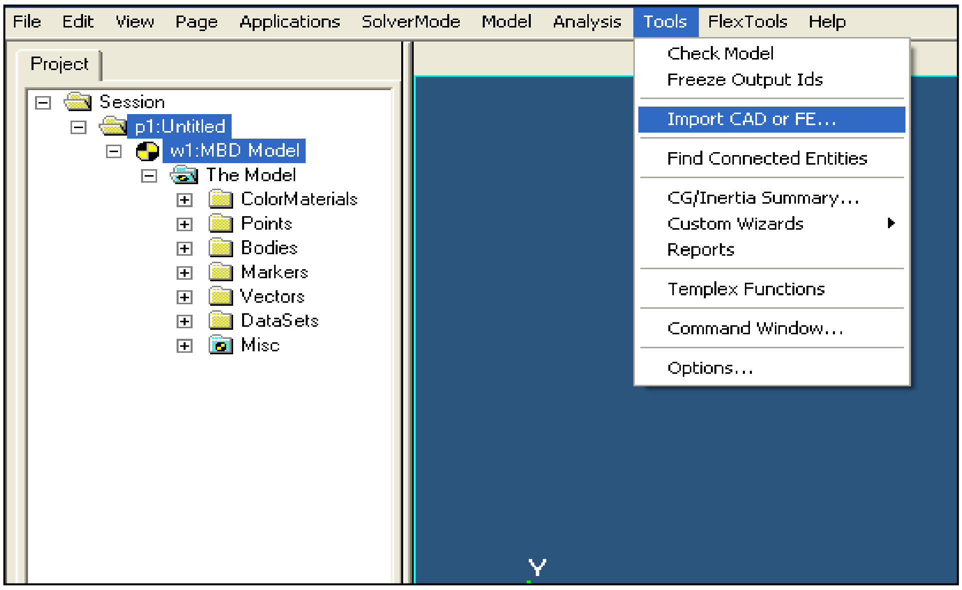

Figure 3.10: H3D file creation

The number of graphic files created depends upon the number of collectors used during the meshing. Graphics of slots are needed independently, for this purpose meshing of slots were done using different collectors. After creating the graphics, all the graphics are attached to the associated bodies. Each graphic is attached by defining the associated body.

3.4.6 Pre- Processing In MotionView

Points

Points are needed to define the centre of gravity locations of objects and joint locations in MotionView. Nine points are created to define the centre of gravity of all the nine components of HVAC. These cg points will be further used to define bodies. Eleven points are created to define the various joints locations. Centre of gravity locations of components are taken from CAD software (Pro-E) and joint locations are taken from Hypermesh. Coordinates of all the points are shown in Table 3.1.

Table 3.1: Coordinate data

	X	Y	Z
Global Origin	0.000	0.000	0.000
cg_cam	4.677	52.409	-3.543
cg_link1	42.653	40.906	36.002
cg_link2	-100.510	41.195	-24.388
cg_link3	-58.950	45.409	-17.832
cg_pin1	44.583	49.409	21.218
cg_pin2	-41.913	49.409	-30.595
cg_pin3	-89.716	39.409	-25.025
cg_door1	36.183	-63.923	37.813
cg_door2	-88.843	-61.591	-2.409
point_cam_revo	0.013	54.794	-0.003
Point_pin1_fix	44.583	43.909	21.218
Point_pin2_fix	-41.913	44.909	-30.595
Point_pin3_fix	-89.716	45.000	-25.025
Point_link1_fix	42.000	36.409	41.000
Point_lin2_fix	-107.000	43.409	-24.000
Point_door1_ball1	42.000	-160.091	41.000
Point_door2_ball1	-107.000	-167.091	-24.000
Point_door1_ball2	42.000	42.000	41.000
Point_doo2_ball2	-107.000	45.000	-24.000
Point_link3_revo	-42.000	44.909	-10.000

Bodies

Bodies are defined at different centre of gravity points using the mass and inertial properties extracted from the CAD software. Nine bodies are defined using the mass and inertial properties extracted from the CAD software. Mass and inertia properties of all the bodies are shown in Table 3.2.

Table 3.2: Mass and inertia properties

	Mass	Ixx	Iyy	Izz	Ixy	Ixz	Iyz
Ground Body	0.000	0.000	0.000	0.000	0.000	0.000	0.000
Body_cam	0.048	18.783	84.648	66.063	0.000	7.423	0.000
Body_link1	0.006	0.549	0.859	0.469	-0.017	0.011	0.133
Body_link2	0.003	0.057	0.329	0.297	0.022	0.014	-0.001
Body_link3	0.008	0.611	3.036	2.460	0.000	-0.294	0.000
Body-pin1	0.001	0.011	0.001	0.011	0.000	0.000	0.000
Body_pin2	0.001	0.011	0.001	0.011	0.000	0.000	0.000
Body_pin3	0.002	0.052	0.005	0.052	0.000	0.000	0.000
Body_door1	0.108	269.733	150.675	407.223	-0.420	28.190	-0.230
Body_door2	0.064	188.889	33.730	183.139	0.000	-16.514	0.000

The points and bodies created in the MotionView are shown in Fig.3.11.

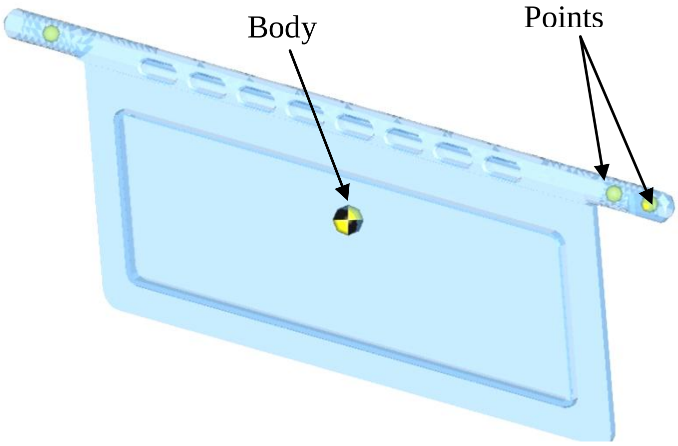

Figure 3.11: Points and bodies created in MotionView

Joints

Joints are defined to constrain the motion of the mechanism, three types of joints are used in the analysis setup these are revolute joint, fixed joint and ball joint. To define a joint we need two bodies between which the joint is needed, a common point and the type of joint. In the pre-processing 11 joints are defined. Four ball joints are provided at the bearing locations where the dampers are supported. Fixed joints are defined to attach the links to the dampers. Pins are fixed to the links by fixed joints. Revolute joints are provided at the cam centre and link3 centre to facilitate the rotation. Fig.3.12 shows the revolute joint created at the cam centre.

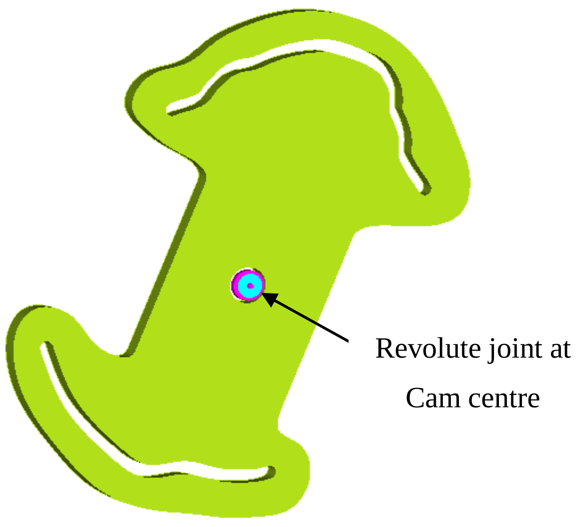

Figure 3.12: Joints created in MotionView

The various joints defined in the analysis setup are:

1. Revolute joint between the cam and ground (cam_revo).
2. Revolute joint between link3 and ground (link3_revo).
3. Fixed joint between link1 and pin1 (pin1_fix).
4. Fixed joint between link3 and pin2 (pin2_fix).
5. Fixed joint between link3 and pin3 (pin3_fix).
6. Fixed joint between link1 and door1 (link1_fix).
7. Fixed joint between link2 and door2 (link2_fix).
8. Ball joint 1 between face damper and ground (door1_ball1).
9. Ball joint 2 between face damper and ground (door1_ball2).
10. Ball joint 1 between foot damper and ground (door2_ball1).
11. Ball joint 2 between foot damper and ground (door2_ball2).

Contact

Contacts are defined between the cam slots and the portion of the lever pin outer surface as shown in Fig.3.13. A suitable value of penalty (3000) and restitution coefficient (0.05) is given for the contacts. Friction is not taken into consideration, as it increases the complexity of the model and thus, the solver time. The penalty value determines the local stiffness properties between the materials. Larger values lead to reduced penetration between two bodies. The coefficient of restitution represents the energy loss between two bodies in contact. A value of 1 represents no energy loss and a perfectly elastic contact.

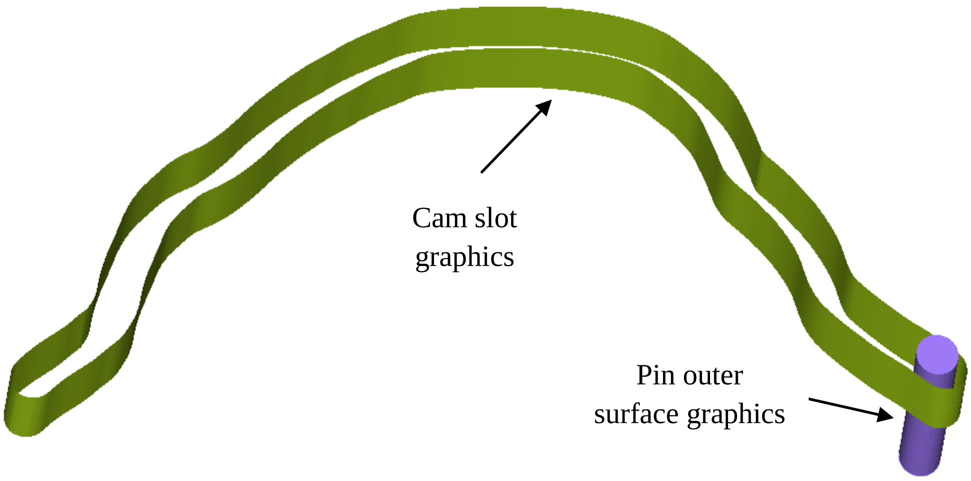

Figure 3.13: Graphics created in MotionView

Graphics are needed to define contact between bodies as the meshing was done using different collectors we have graphics of slot1, slot2 and slot3 independently.

The various contacts defined in the MotionView 9.0 are:

1. Poisson Contact between slot1 and pin1(slot1_pin1).
2. Poisson Contact between slot2 and pin2 (slot2_pin2).
3. Poisson Contact between slot3 and pin3 (slot3_pin3).

Motion

Initial motion is required to simulate the model, after defining all the joints a rotational motion of 10°/sec is defined at the cam revolute joint using the expression"$10D \times \mathrm{TIME}$". With this expression if the analysis is run for 5 seconds then the cam will rotate through $50°$.

Outputs

Outputs are defined for cam rotation, doors rotation and torque required to operate the cam. Markers are required to define outputs. A marker is a coordinate system attached to a body that is used as a reference for applied loads and output requests. To define a marker, things to be specified are the associated body, the origin of the marker, and the axes' rules for the marker. Six markers are defined to produce the required outputs:

1. Marker defined at a point on rotational axis of cam with ground body (cam_g).
2. Marker defined at a point on rotational axis of cam with cam body (cam_b).
3. Marker defined at a point on the rotational axis of face damper with ground body (door1_g).
4. Marker defined at a point on the rotational axis of face damper with ground body (door1_b).
5. Marker defined at a point on the rotational axis of foot damper with ground body (door2_g).
6. Marker defined at a point on the rotational axis of foot damper with foot damper body (door2_b).

With these markers taken as reference, four outputs are defined for cam toque, cam rotation, door 1 rotation and door 2 rotations. For the rotational output of cam and doors expression 'AY({id string of ground body marker},{id string of component body marker})*rtod' has been used. In the expression "AY" denotes angular output about global Y axis. As on each point on the rotational axis two markers has been defined one with ground body and other with component body, in the braces the id strings of these two markers are taken. In expression “rtod” denotes conversion of degrees into radians.

1. Output defined for cam toque (cam_torque).
2. Output defined for cam rotation (cam_rot).
3. Output defined for foot damper rotation (door1_rot).
4. Output defined for face damper rotation (door2_rot).

After doing the preprocessing and resolving the errors the model is submitted for the Multibody analysis in Motion Slove 9.0.

3.4.7 Solution

The solver (MotionSolve) is run for an end time of 8s, using the ABAM integrator type, and the outputs obtained are plotted using HyperGraph from the HyperWorks 9.0 suite. The workstation used for the analysis has 3960 MB RAM, and a CPU speed of 2530 MHz.

3.4.8 Post Processing

The following outputs are obtained for HVAC kinematic mechanism:

(a) Foot damper rotation as a function of cam rotation.

(b) Face damper rotation as a function of cam rotation.

(c) Torque as a function of cam rotation.

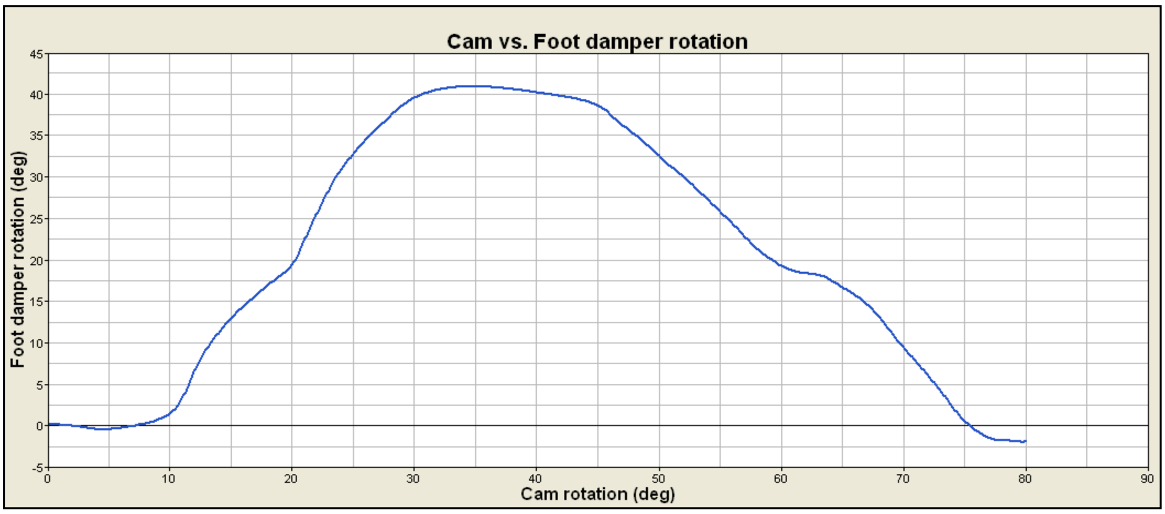

Figure 3.14: Cam vs. Foot damper rotation

As can be seen from Fig.3.14 and 3.15, there is an optimal level of door rotation for a given cam rotation angle. The door rotation should not be very high (as it will lead to high torque values) or very low, because sufficient level of air flow in a given time could not be achieved.

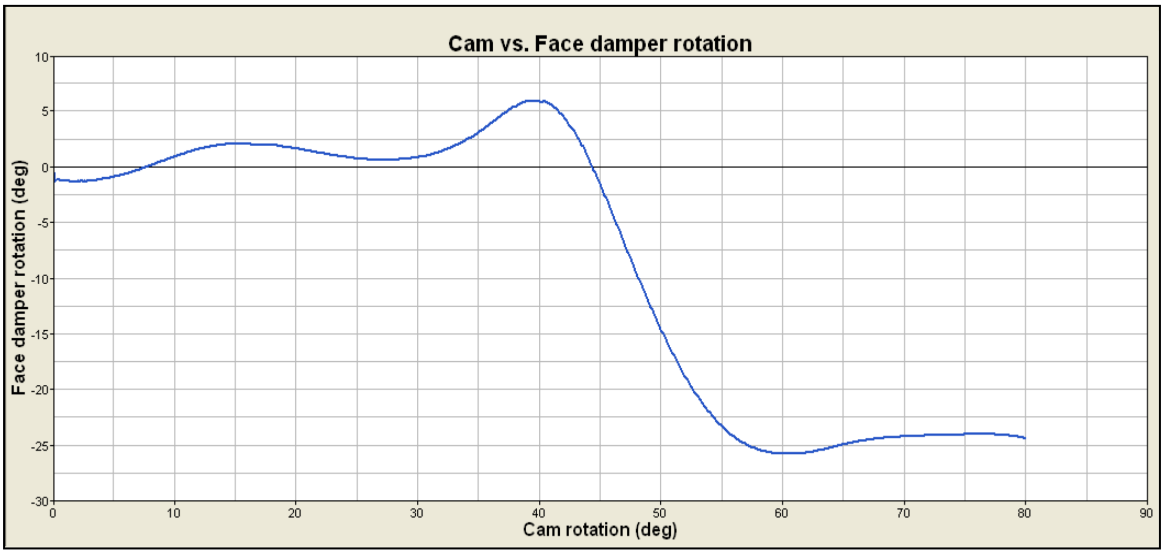

Figure 3.15: Cam vs. Face damper rotation

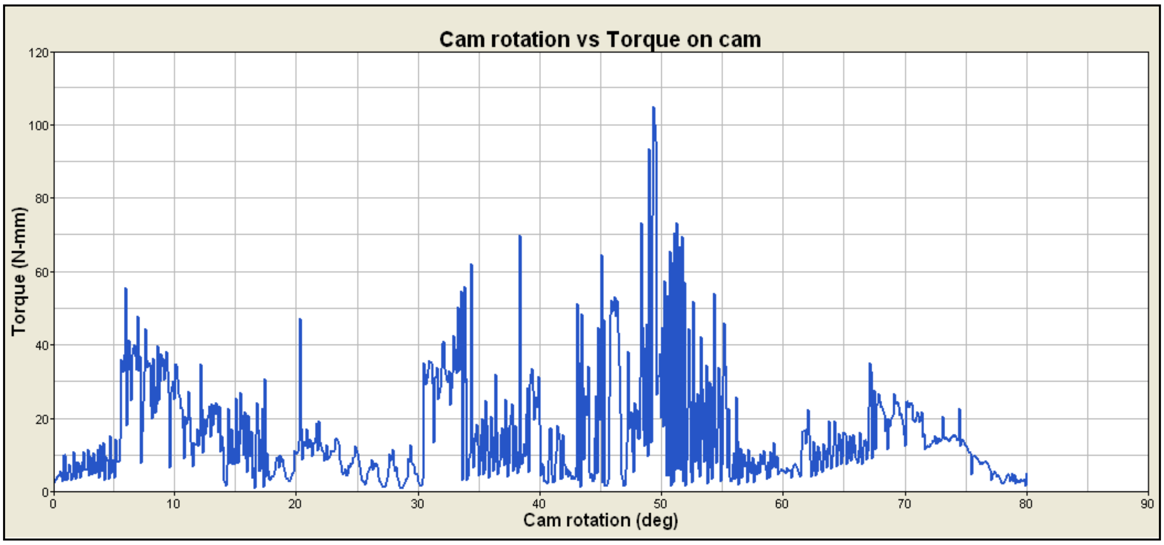

Figure 3.16: Cam rotation vs. Torque on cam

As can be seen from Fig.3.16, there are spikes in the torque graph because the cam slots are not so smooth due to the reverse engineering of the cam.

CHAPTER 4

CAM DESIGN

4.1 CAM MECHANISMS

The transformation of one of the simple motions, such as rotation, into any other motions is often conveniently accomplished by means of a cam mechanism A cam mechanism usually consists of two moving elements, the cam and the follower, mounted on a fixed frame. Cam devices are versatile, and almost any arbitrarily-specified motion can be obtained. In some instances, they offer the simplest and most compact way to transform motions.

A cam may be defined as a machine element having a curved outline or a curved groove, which, by its oscillation or rotation motion, gives a predetermined specified motion to another element called the follower. The cam has a very important function in the operation of many classes of machines, especially those of the automatic type, such as printing presses, shoe machinery, textile machinery, gear-cutting machines, and screw machines. In any class of machinery in which automatic control and accurate timing are paramount, the cam is an indispensable part of mechanism. The possible applications of cams are unlimited, and their shapes occur in great variety.

4.2 CAM NOMENCLATURE

Different cam nomenclature, shown in Fig.4.1, is defined as following:

a) **Trace point:** A theoretical point on the follower, corresponding to the point of a fictitious knife-edge follower. It is used to generate the pitch curve. In the case of a roller follower, the trace point is at the centre of the roller.
b) **Pitch curve:** The path generated by the trace point at the follower is rotated about a stationary cam.
c) **Working curve:** The working surface of a cam in contact with the follower. For the knife-edge follower of the plate cam, the pitch curve and the working curves coincide. In a close or grooved cam there is an inner profile and an outer working curve.
d) **Pitch circle:** A circle from the cam centre through the pitch point. The pitch circle radius is used to calculate a cam of minimum size for a given pressure angle.

e) **Prime circle (reference circle):** The smallest circle from the cam canter through the pitch curve.

f) **Base circle:** The smallest circle from the cam centre through the cam profile curve.

g) **Stroke or throw:** The greatest distance or angle through which the follower moves or rotates.

h) **Follower displacement:** The position of the follower from a specific zero or rest position (usually it is the position when the follower contacts with the base circle of the cam) in relation to time or the rotary angle of the cam.

i) **Pressure angle:** The angle at any point between the normal to the pitch curve and the instantaneous direction of the follower motion. This angle is important in cam design because it represents the steepness of the cam profile.

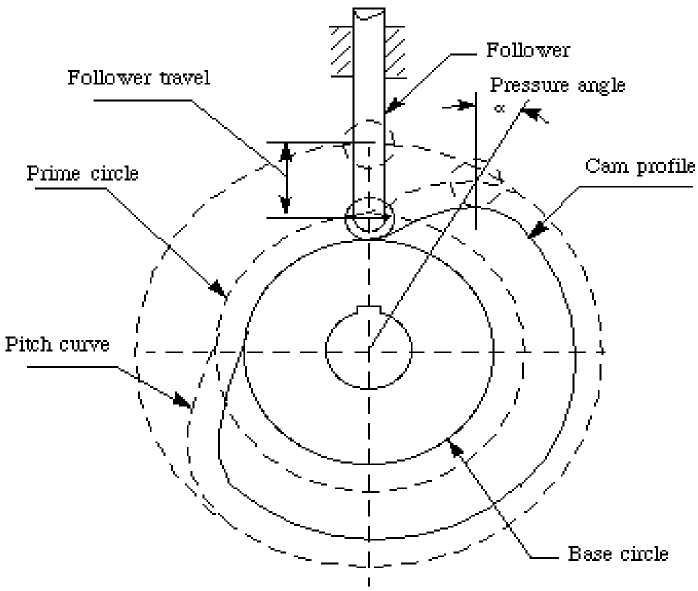

Figure 4.1: Cam Nomenclature

4.3 HVAC CAM DESIGN

The outputs obtained from the multibody analysis of HVAC kinematic mechanism gives information about the relative motion of links with respect to the cam rotation, mechanism cam can be designed by oscillating link method given in books.

The cam is designed with the following specifications:

(a) Follower to dwell for the first 12° cam rotation.

(b) Follower to move inwards through an angular displacement of $45°$ during the next $15°$ rotation of the cam.

(c) Follower to dwell for the next $20°$ rotation of the cam.

(d) Follower to move inward through an angular displacement of $45°$ during the next $20°$ rotation of the cam.

(e) Follower to dwell during the next $6°$ rotation of cam.

The length of the follower is 30 mm; horizontal distance between the pivot centre and cam axis $= 66.5$ mm; minimum radius of cam$=$ $49.5\ mm$; follower moves with uniform velocity. The two methods of cam design are explained in detail in the following sections.

4.3.1 Method 1

CAD software has been used to design the cam profile by a well defined method [11]. This method is described in detail below:

The angular displacement of follower is $90°$ ($\pi/2$ rad), length of arc $= 30 \text{ x } \pi/2 =$ 47.1239 mm. So, the height of the displacement diagram taken is 47.1239 mm. Displacement diagram is shown in Fig.4.2.

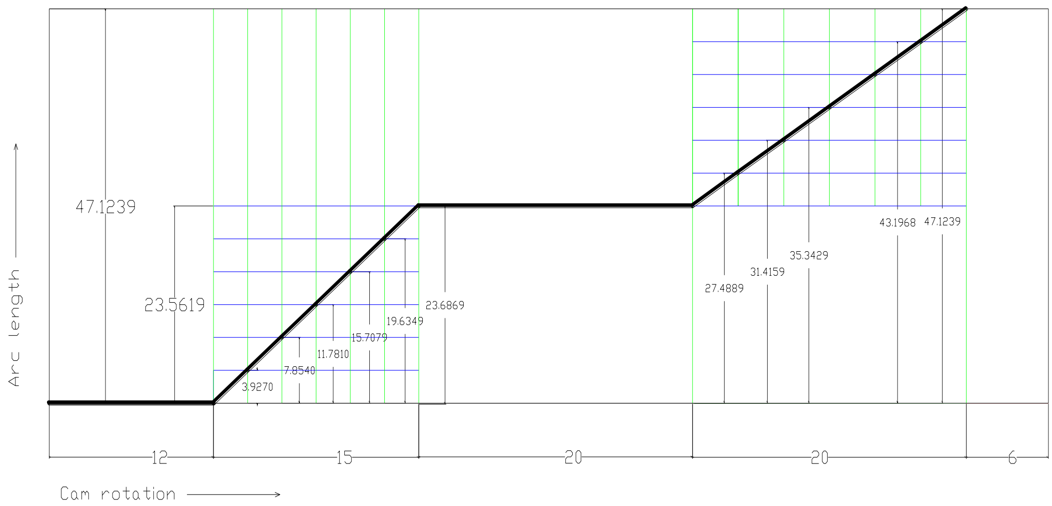

Figure 4.2: Displacement diagram

Procedure

1. First of all draw a prime circle with centre o and radius equal to the minimum radius of the cam (49.5 mm).
2. Now locate the follower as shown in the Fig.4.3.

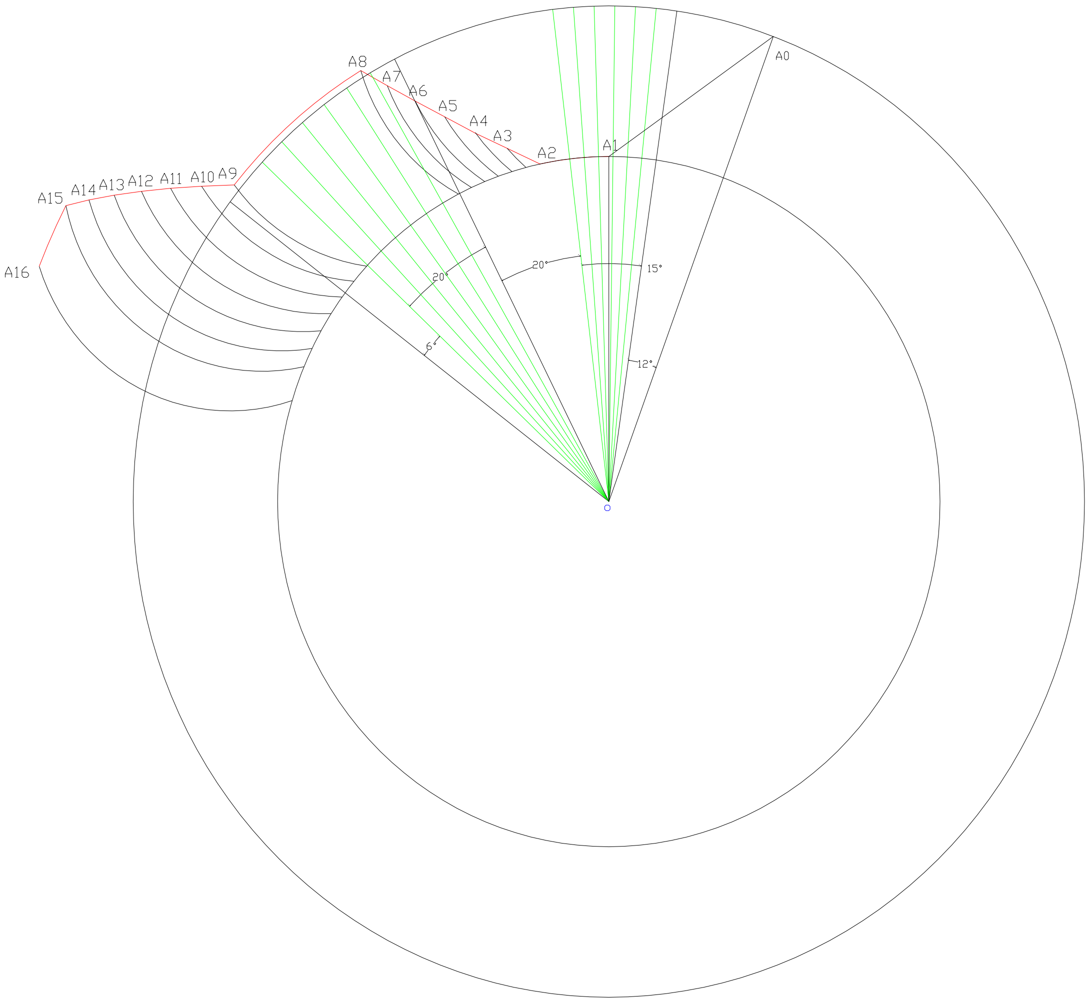

Figure 4.3: Cam profile by Method 1

3. JoinOA_0. Draw angle $A_OOM = 12°$ to represent the dwell, angle $MON = 15°$ to represent the inward stroke of the follower, angle $NOP = 20°$ to represent the dwell, angle $POQ = 20°$ to represent the next inward stroke, angle $QOR = 6°$ to represent the next dwell.
4. Divide angles MON and POQ into the same number of equal parts as in the displacement diagram.
5. Now with these points draw arcs of 30 mm radius to intersect the prime circle.
6. Set the lengths of arcs equal to the distance measured from the displacement diagram.
7. Join the end points of arcs with a smooth curve to make the cam profile.

4.3.2 Method 2

This method is simple and fast as compared to the method 1 as there is no need of displacement diagram and measurement of arc lengths. In method 1 only one slot can be drawn on a single page, drawing two slots on a single page makes the diagram complicated and there are chances of errors. By using different layers in AutoCAD, two slots can be drawn, but it consumes more time and there are chances of human errors in creating the arc lengths from displacement diagram. So a new simplified method has been developed to create the slot profiles. With this method more than one slot profile can be easily drawn on a single page, without using different layers and without using displacement diagrams. The cam profile created by method 2 is shown in Fig.4.4.

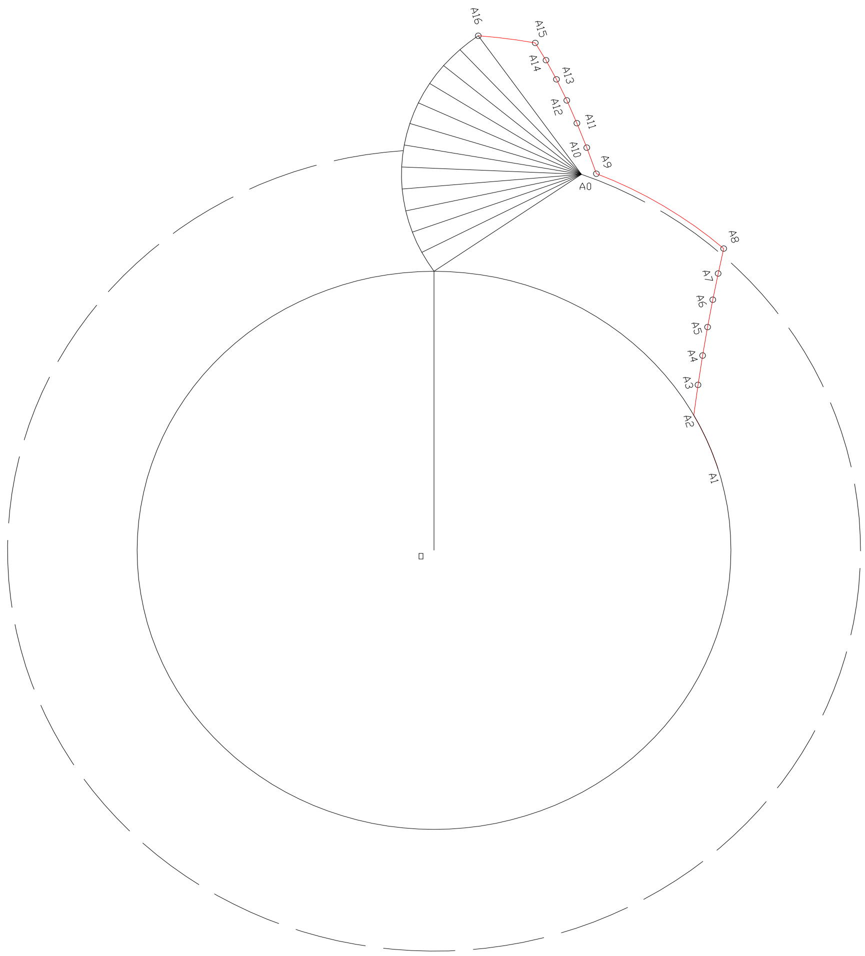

Figure 4.4: Cam profile by Method 2

Procedure

1. First of all draw a prime circle with centre O. (Prime circle radius $= 49.5mm$).
2. Now locate the position of link as shown in the Fig.4.5. (link length $= 30mm$)
3. Draw an arc of 90°, radius equal to the link length in clockwise direction with starting point A_1 .
4. Then divide the arc into 12 equal parts as shown in the Fig.4.5.
5. For first 12° dwell, rotate the starting point by 12° clockwise and then create an arc of 12° radius equal to base radius from point A_1 to point A_2.
6. Rotate the arc by 2.5° clockwise and join the arc end to the 7.5° position of the link. Similarly rotate the profile by next 2.5° and join the profile end to the next position of link till the 45° position of the link.
7. For second 20° dwell rotate the profile by 20° and create an arc of 20° with centre o and radius equal to OA_8 from point A_8 to point A_9.
8. Rotate the profile by 20° in 6 steps and join the profile end points to the respective 6 positions of the link after each rotation.
9. Then rotate the profile by 6° and create an arc of 6° with centre O and radius OA_{15} from point A_{15} to point A_{16}.
10. Finally rotate the profile by 73° anticlockwise.

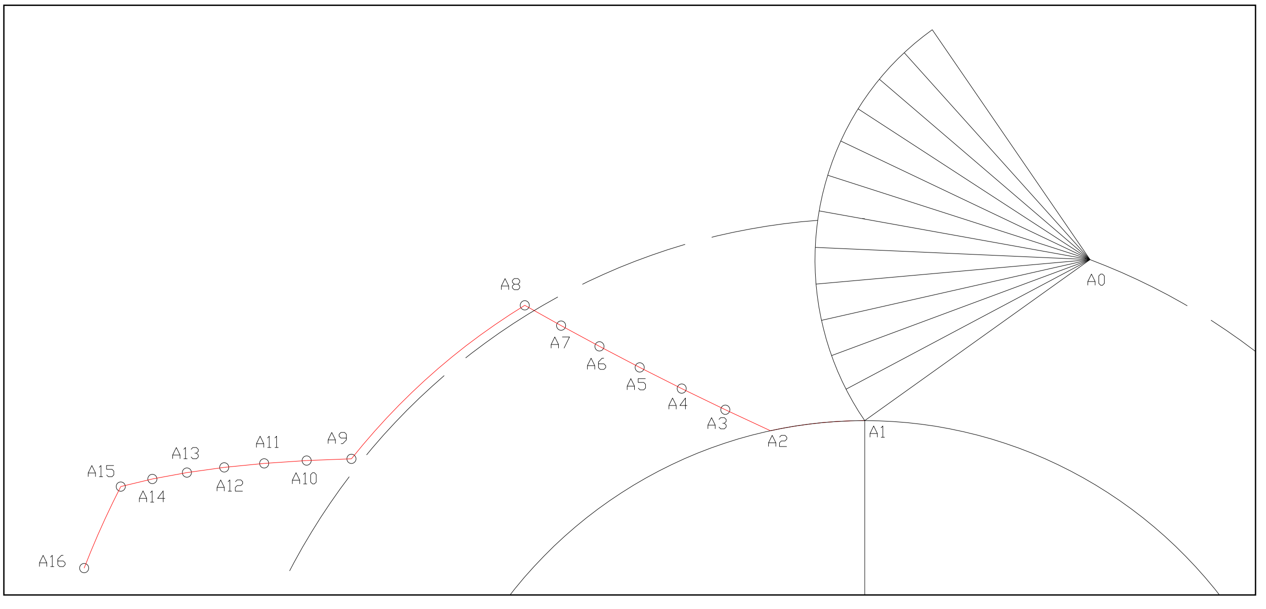

Figure 4.5: Final cam profile

Advantages

1) Takes less time as compared to method 1.
2) Procedure is simple and less complicated
3) No need of displacement diagram.
4) Both slot profiles can be drawn on a single page easily.

To compare the two methods, two cams were designed for the same output with the two methods and the analysis was done in the Motion View 9.0. Results obtained from both the methods are same as can be seen from Fig.4.6.

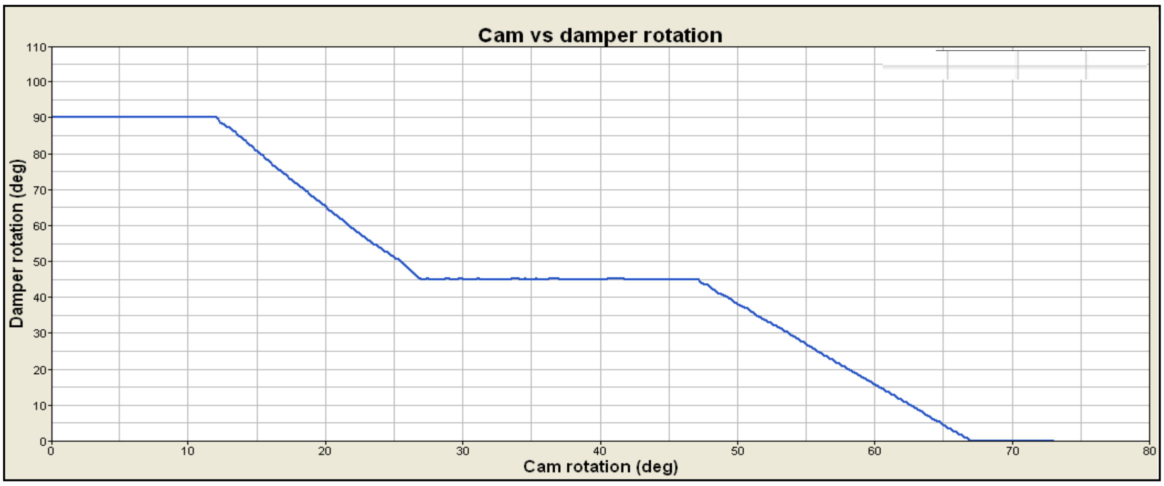

(a)

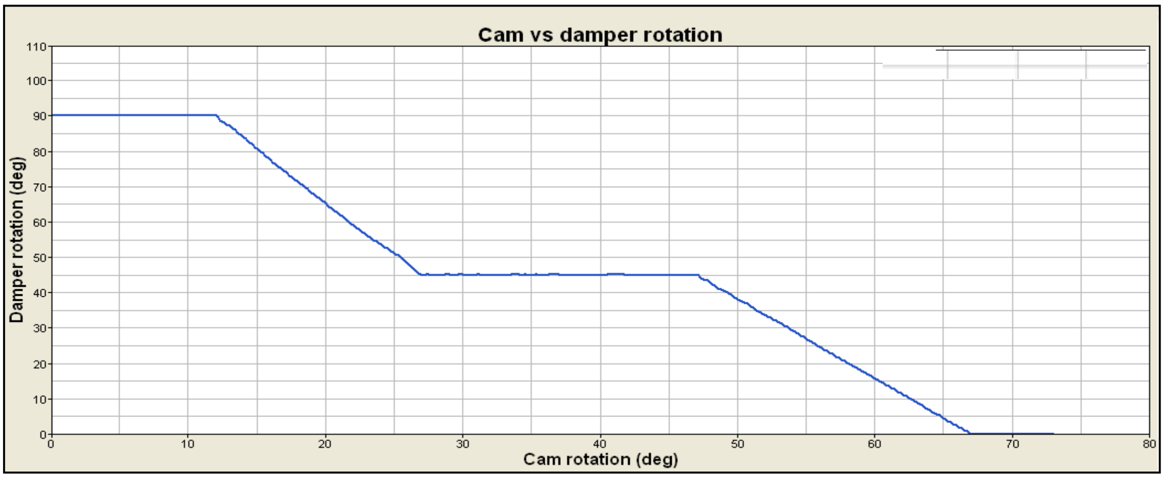

(b)

Figure 4.6: Comparison of Two Methods

(a) Output obtained from Method 1; (b) Output obtained from Method 2

4.4 MODEL- A CAM DESIGN

In the reverse engineered HVAC mechanism, the cam slots were made by tracing the slots on a paper and then points were marked over and measured with respect to a reference frame. The measurement was done with the drafter scale, so the slots were not accurate; they were made with the approximate data. The output graphs obtained from the simulation are irregular and also the average torque required to operate the cam is not clear from the torque graph. From the displacement plots, various positions of the doors with respect to the cam rotation are obtained and total angular displacement of dampers are measured from the HVAC module, with this data as an input a new cam has been designed. Using the methodology described earlier, simulation of the mechanism with the new cam has been done, the displacement curves obtained are smoother and also the average torque required to operate the cam is clear from the torque graph.

Cam design data obtained:

Total angular rotation of face damper $= 41°$

Total angular rotation of foot damper $= 38°$

Angular rotation of link3 $= 15°$

Foot mode specifications:

(a) Dwell for 7° rotation of cam

(b) 19° upward angular displacement of link for the next 13° rotation of cam.

(c) Dwell for next 8° cam rotation.

(d) 22° upward stroke for next 12° rotation of cam.

(e) Dwell for the next 13° cam rotation.

(f) 22° downward stroke for next 15° rotation of cam.

(g) Dwell for next 3° cam rotation.

(h) 19° downward stroke for the next 14° cam rotation.

(i) Dwell for the next 3° of cam rotation.

Face mode specifications:

(a) Dwell for 40° rotation of cam.

(b) 38° downward stroke for the next 20° cam rotation.

(c) Dwell for next 20° rotation of cam.

4.4.1 Cam design

The cam of the mechanism is designed by method 2, described in the previous section. Fig.4.7 shows the profile of cam slots.

Specifications of cam:

Prime circle diameter for foot mode = $49.5\ mm$.

Prime circle diameter for face mode = $49.2\ mm$.

Face mode link length (link 1) = $20\ mm$.

Foot mode link length (link 3) = $20.5\ mm$.

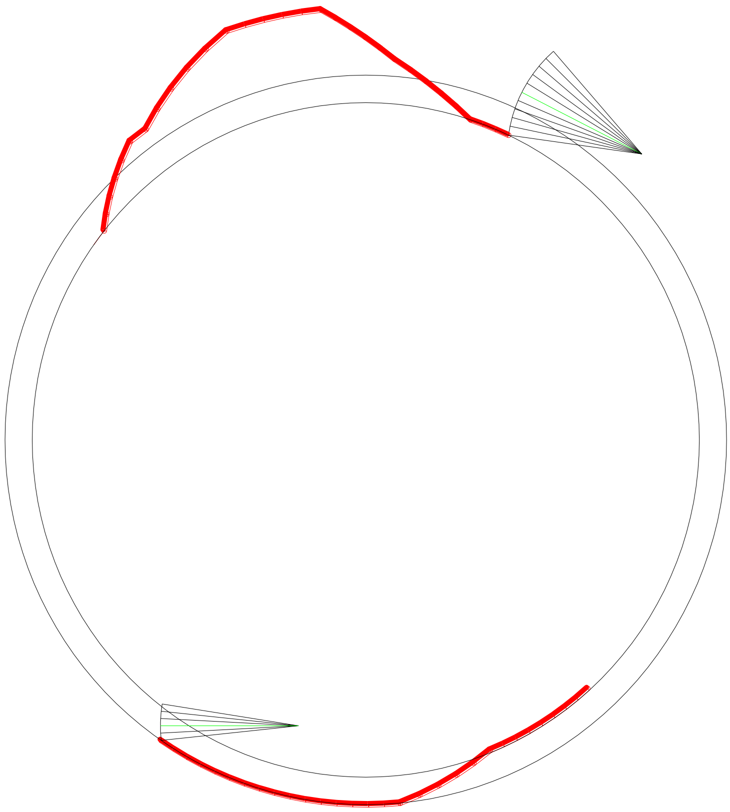

Figure 4.7: Cam profile

4.4.2 Output results

To simplify the model cam slots are made with small rounds at the edges, large rounds increases the mesh size of contact surfaces which leads to the interference of contacting surfaces and the analysis becomes unstable. Analysis is done with $0.3\ mm$ mesh size of contact surfaces. The output results *i.e.* damper rotation *w.r.t.* cam rotation are shown in Fig.4.8 and 4.9. The cam rotation *w.r.t.* torque on cam is shown in Fig.4.10.

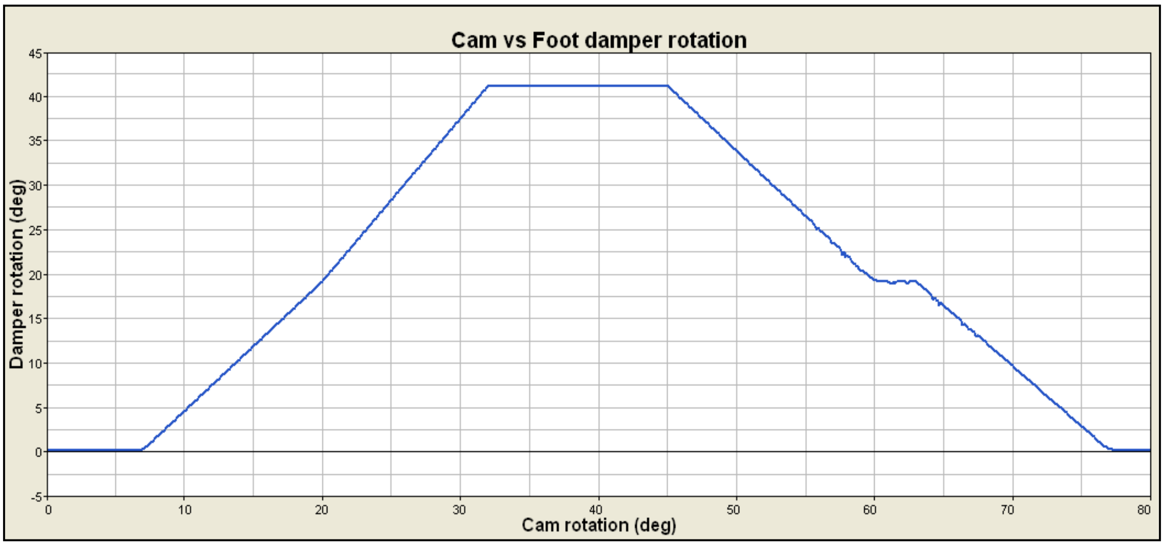

Figure 4.8: Cam vs. Foot damper rotation

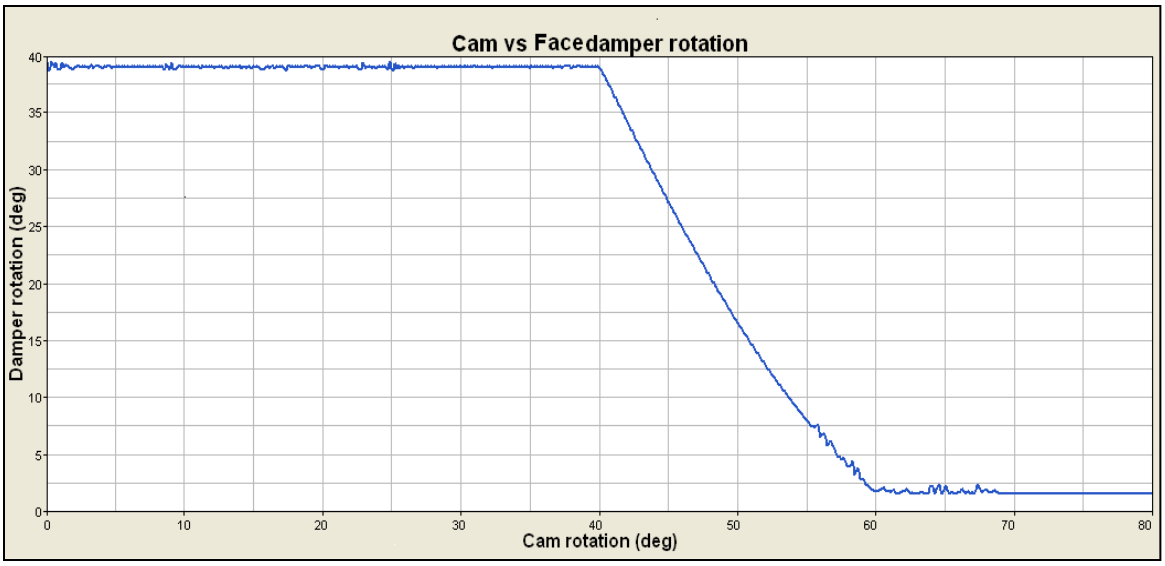

Figure 4.9: Cam vs. Face damper rotation

Small irregularities in the displacement graphs are due to the value set for the penalty, smooth plots can be obtained with smaller values of penalty but it would increase the spikes in the torque graph. So a suitable penalty value of 3000 is taken.

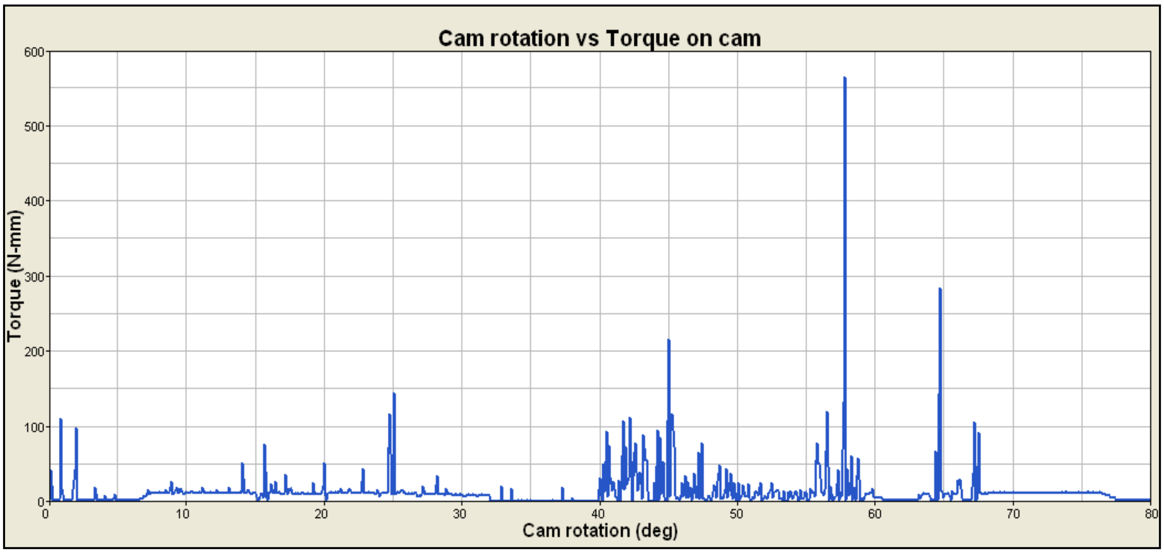

Figure 4.10: Cam rotation vs. Torque on cam

A line at the bottom of the torque graph, Fig.4.10, shows that the average torque required to operate the cam is $11\ N - mm$. Spikes in the graph are due to the inertial effects and the mesh size taken for the contact surfaces. These spikes can be reduced by taking smaller mesh size, which requires high configuration computer to solve the analysis, but the average torque required would remain same. Smaller mesh size can make the average torque line clearer in the graph.

CHAPTER 5

HVAC KINEMATIC MECHANISM DESIGN

5.1 INTRODUCTION

HVAC kinematic mechanism design is one of the crucial step in the design process of the complete module. Design should be compact and torque required to operate the cam should not be high. Base radius of the cam in the mechanism should be taken according to the space available. For the desired output results two mechanisms have been designed for the same dampers location and a comparison is made between the two designs. The assumptions include a constant angular velocity of the cam, and the rigidity of the parts in the mechanism. The movements of various parts have been analyzed using the animation in HyperView 9.0. The other important outputs include the displacement and torque graphs plotted with the use of HyperGraph 9.0.

5.2 PROBLEM

The problem is to design a HVAC kinematic mechanism with the following specifications:

Foot mode specifications:

a) Dwell for 3° rotation of cam
b) 45° Upward angular displacement of link for the next 17° rotation of cam.
c) Dwell for next 8° cam rotation.
d) 16° upward stroke for next 9° rotation of cam.
e) Dwell for the next 6° cam rotation.
f) 31° downward stroke for next 9° rotation of cam.
g) Dwell for next 8° cam rotation.
h) 30° downward stroke for the next 10° cam rotation.
i) Dwell for the next 3° of cam rotation.

Face mode specifications:

a) Dwell for 6° rotation of cam.
b) 45° downward stroke for the next 20° cam rotation.
c) Dwell for next 20° rotation of cam.

d) 45° downward stroke for the next 15° cam rotation.

e) Dwell for next 15° rotation of cam.

5.3 KINEMATIC MECHANISM DESIGN

Two designs have been made for the required output:

(1) Two link kinematic design

(2) Three link kinematic design

5.3.1 Three link HVAC kinematic design

The CAD geometry which is used as an input for the analysis is shown in the Fig.5.1.

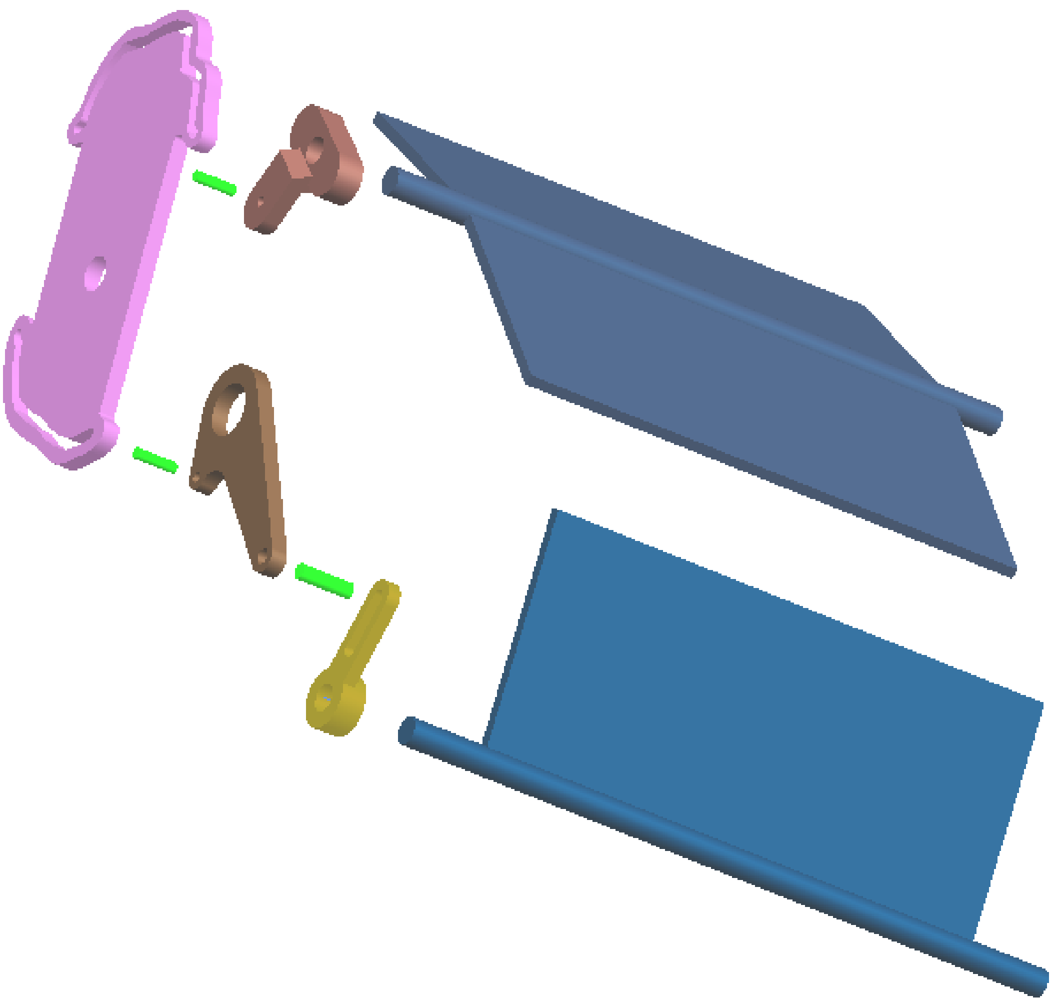

Figure 5.1: Exploded view of Assembly

Cam Design

The cam for the mechanism is designed by method 2, described in the previous chapter. Profile of cam slots are shown in Fig.5.2.

Specifications of cam:

Prime circle diameter for foot mode = $49.5\ mm$.

Prime circle diameter for face mode = $35\ mm$.

Foot mode link length (link 1) = $20\ mm$.

Face mode link length (link 3) = $20\ mm$.

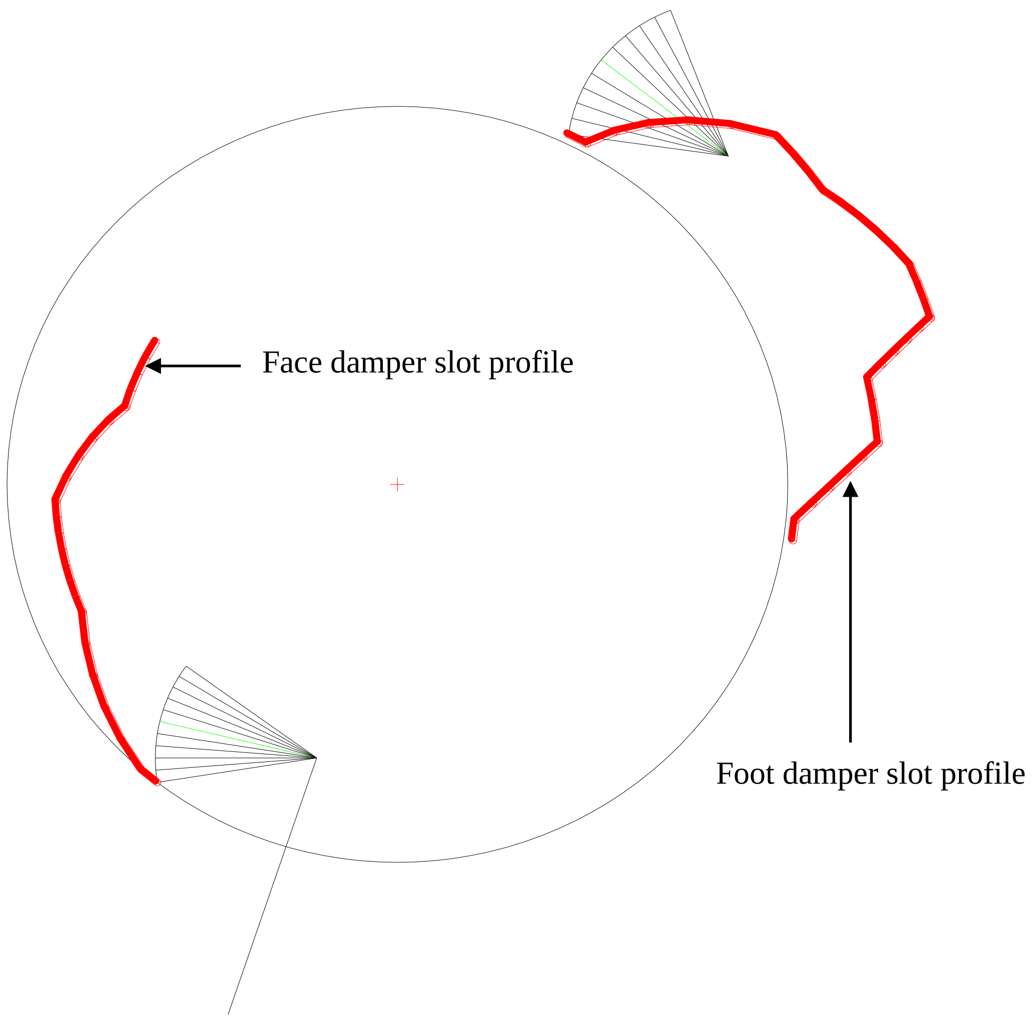

Figure 5.2: Cam profile

Link design

For foot damper movement one link is used, two links are used for the face damper movement. The design of the two links for the face mode was done by the graphical method described below:

Total angular displacement of face damper is 90°, the cam is designed for the 45° angular displacement of link 3. 90° movement of face damper is achieved by relative motion between the link 3 and link 2.

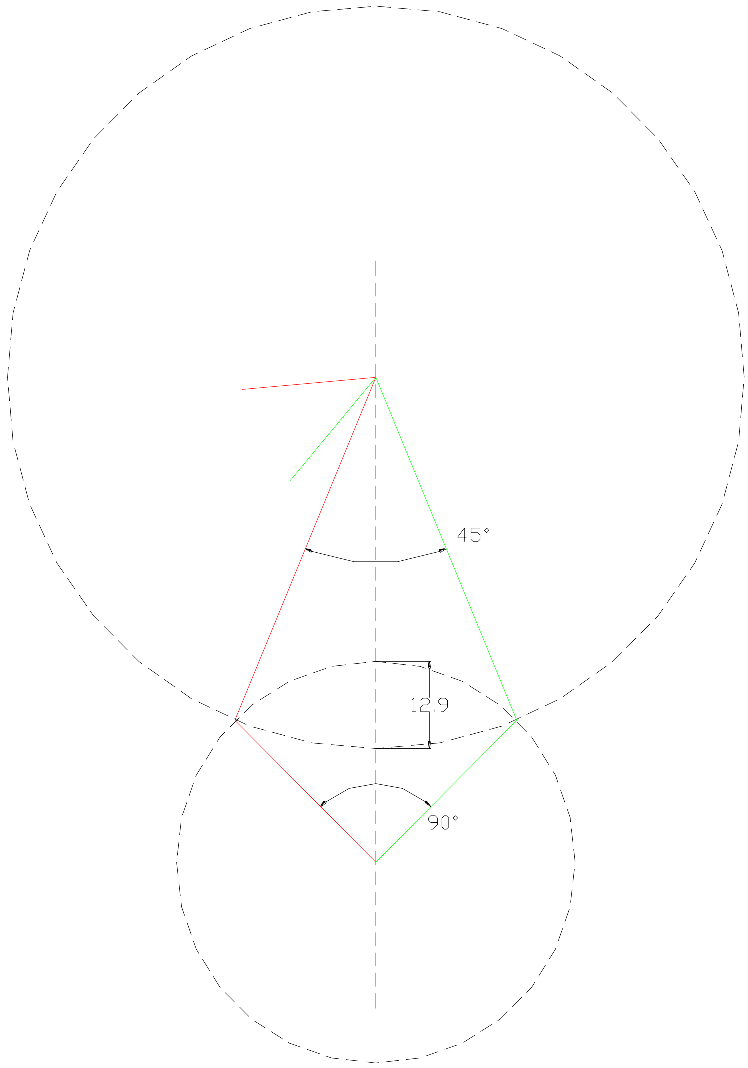

Figure: 5.3 Graphical method of Link Design

In the Fig.5.3, green colour shows the initial positions of link 3 and link 2 and red colour shows the final position. Graphically the length of link 2 slot and the position of pin 3 are obtained. Link 2 slot length is taken more than 12.9 mm.

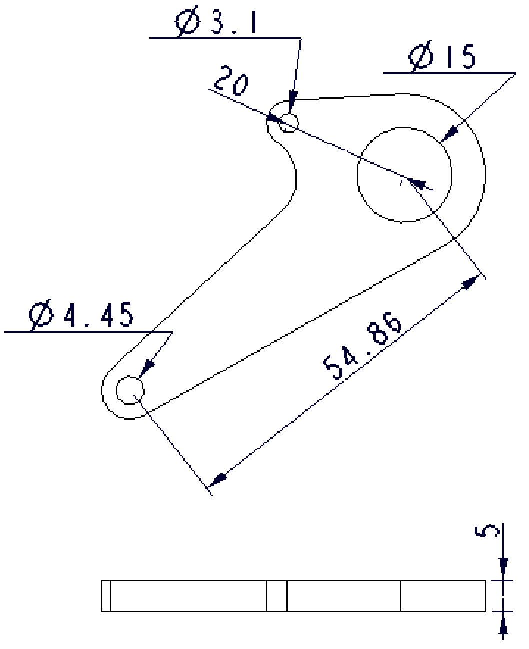

Link 3

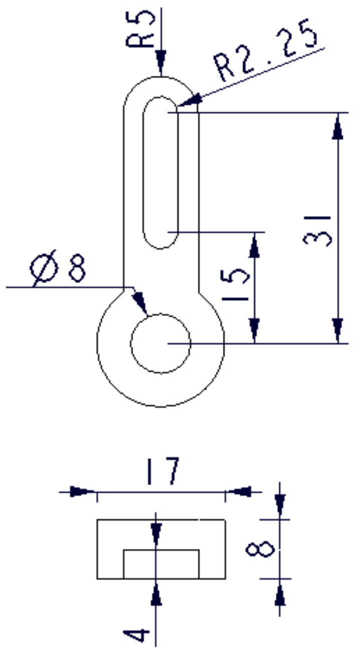

Link 2

Figure 5.4: Component Drawings

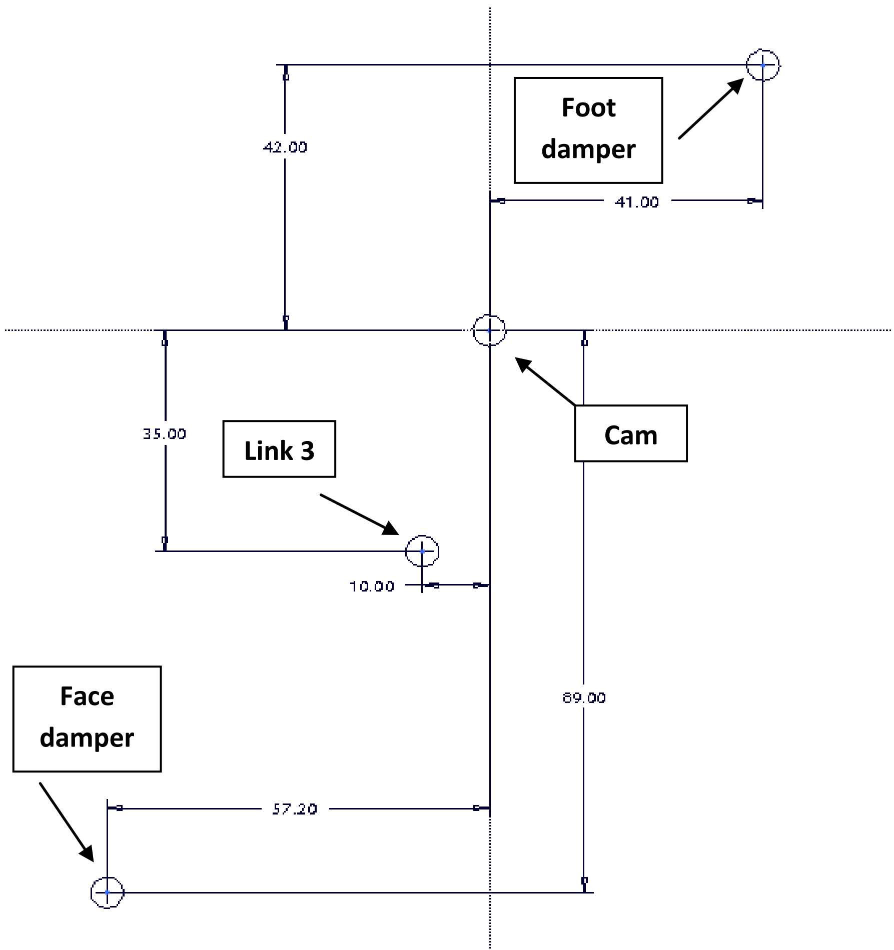

Figure 5.5: Component centre locations

Drawings of link 2 and link 3 are shown in Fig.5.4. Fig.5.5 shows the component centre locations. Dimensions of Link1, Foot damper, Face damper and pins are same as were in Model- A. Using the methodology described earlier, the analysis has been run for 73° of cam rotation. The outputs obtained *i.e.* damper rotation *w.r.t.* cam rotation are shown in Fig.5.6 and 5.7. The cam rotation *w.r.t.* torque on cam is shown in Fig.5.8.

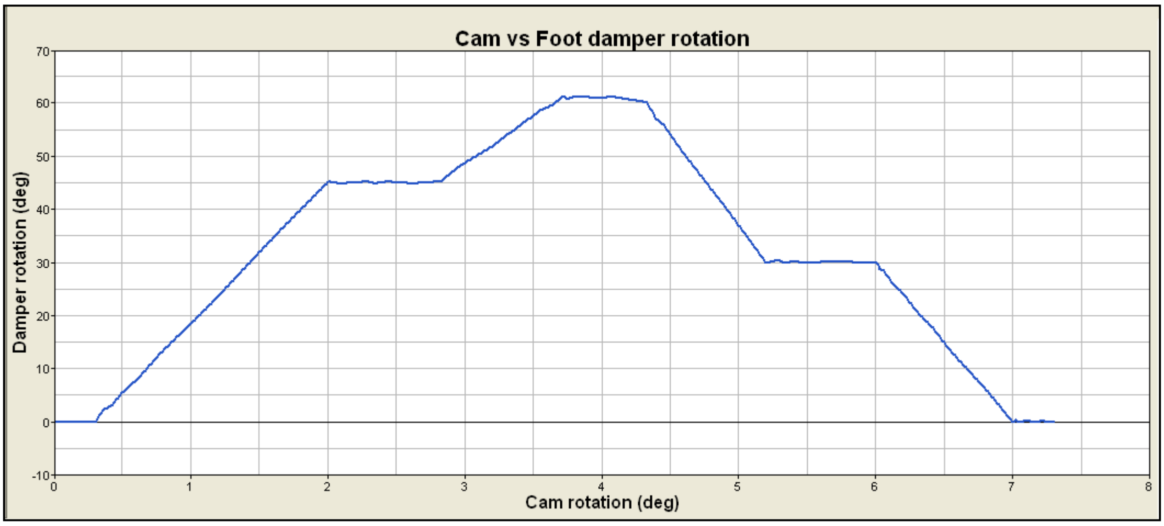

Figure 5.6: Cam vs. Foot damper rotation

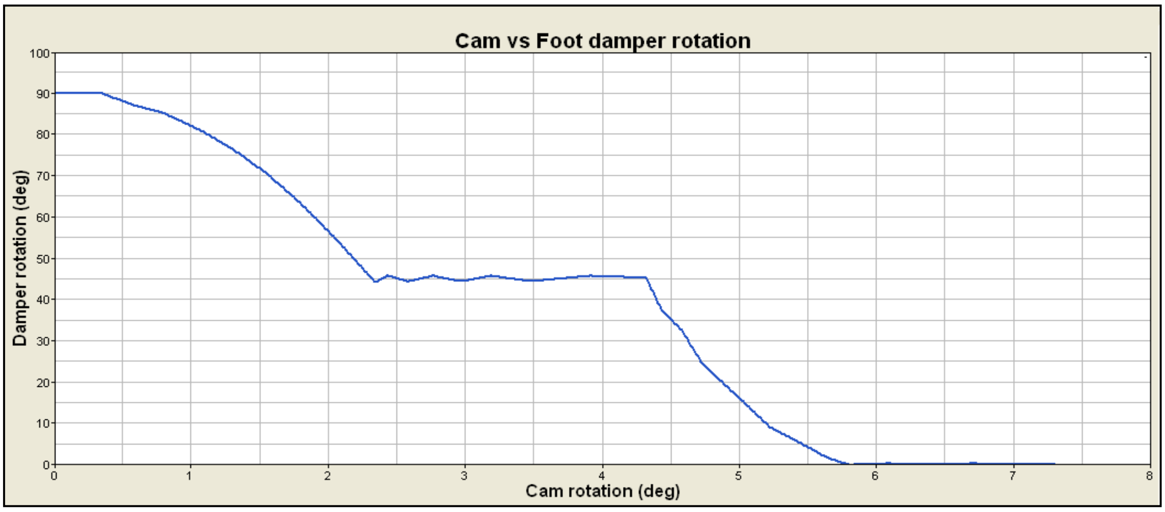

Figure 5.7: Cam vs. Face damper rotation

Displacement curve is obtained for the 73° rotation of the cam. The cam slots are made smoother, i.e., without any sharp edges so that there is no obstruction to the movement of the pins inside those slots. After a few iterations, displacement graphs of the mechanism shown in Fig.5.6 and 5.7 have been reached.

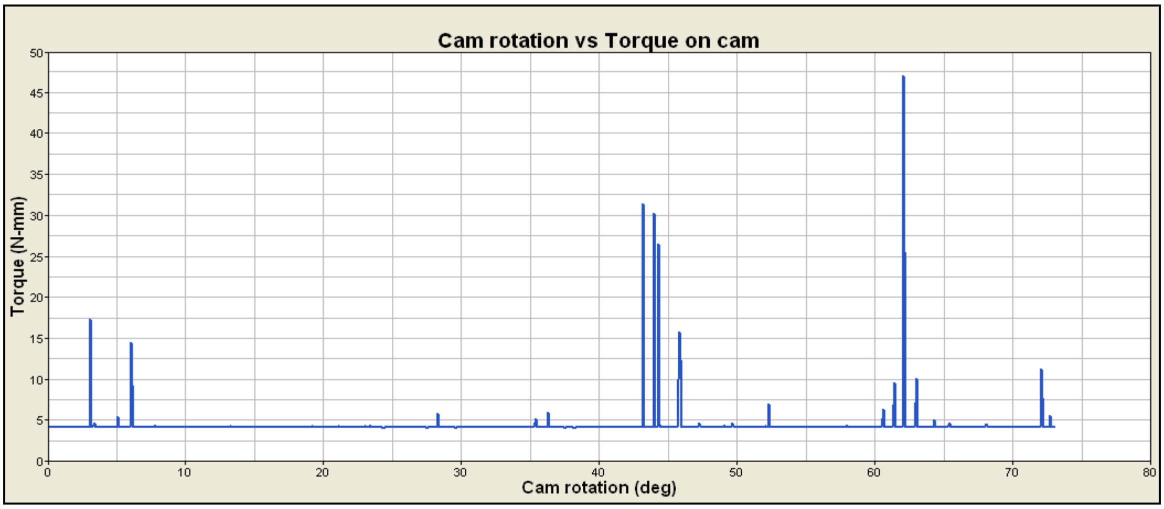

Figure 5.8: Cam rotation vs. Torque on cam

The average torque required to operate the cam is $4.5\ N - mm$. The spikes in the torque graph, Fig.5.8, are due to the inertial effects and mesh size taken for the contact surfaces. With the available computer configuration mesh size cannot be taken less than $0.2\ mm$ as the analysis becomes unstable below 0.2 mm mesh size.

5.3.2 Two link HVAC kinematic design

In this mechanism one link is used to operate the foot damper. Damper locations and cam locations are taken same as were in three link mechanism. The CAD geometry which is used as an input for the analysis is shown in the Fig.5.9.

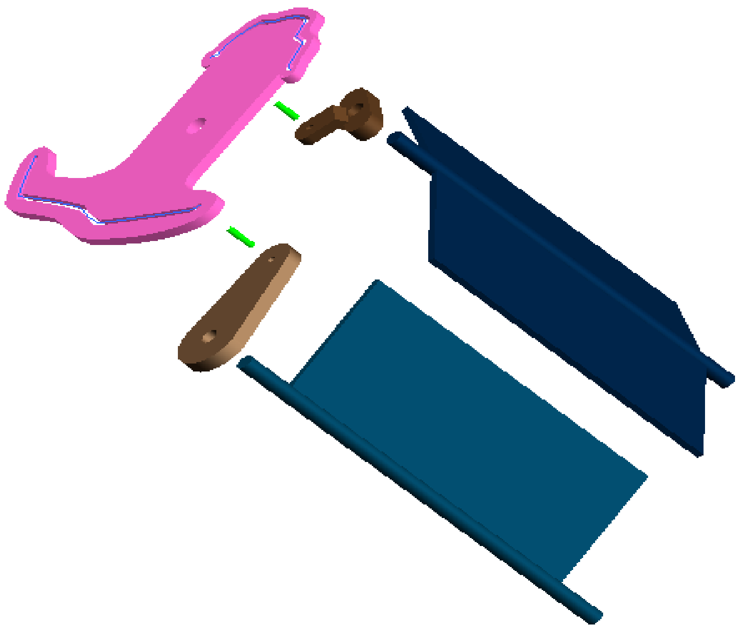

Figure 5.9: Exploded view of Assembly

Cam specifications:

Prime circle radius for foot mode = $49.5\ mm$.

Prime circle radius for face mode = $65.6\ mm$.

Link 1 length = $20\ mm$.

Link 2 length = $48\ mm$.

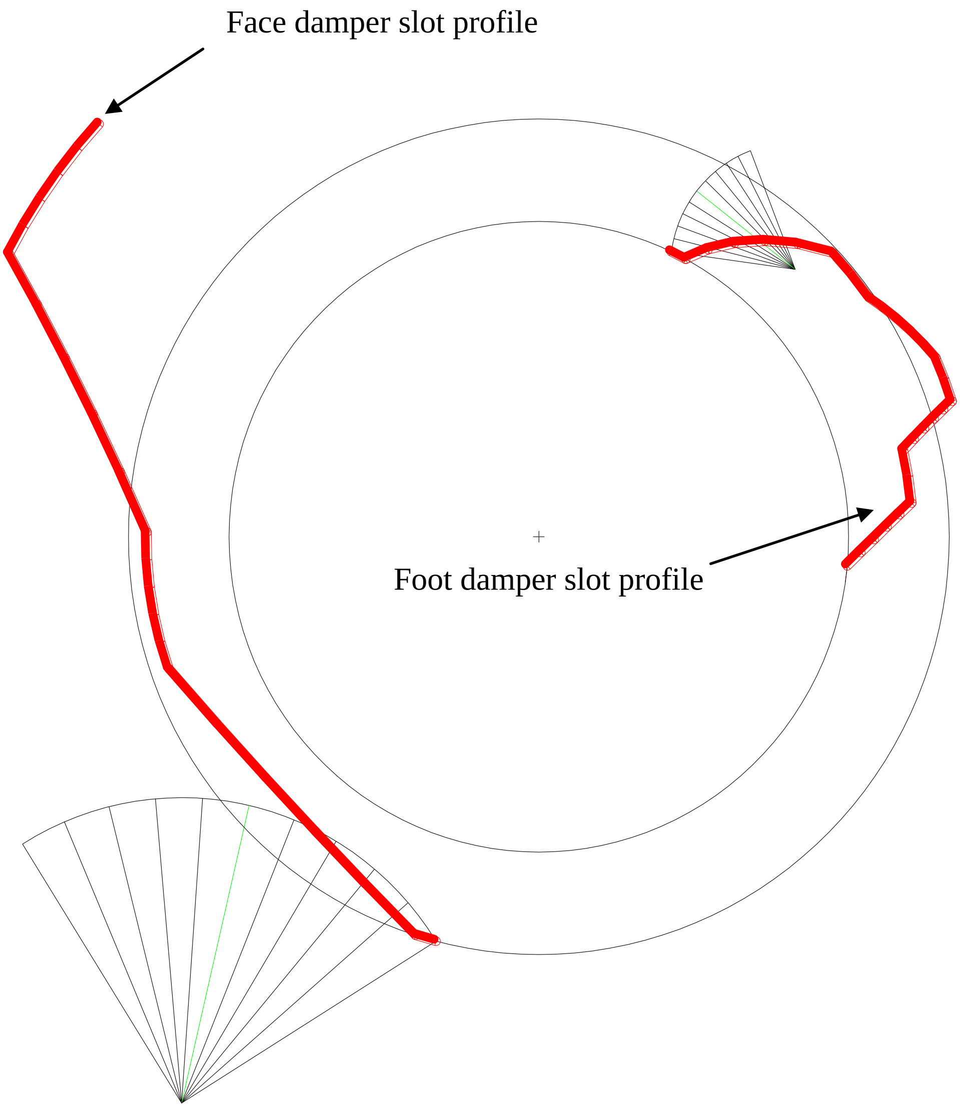

Figure 5.10: Cam profile

Fig.5.10 shows the profile of cam slots.

Using the methodology described earlier, the analysis has been run for 73° of cam rotation.The outputs obtained *i.e.* the damper rotation *w.r.t.* cam rotation and torque required to operate the cam are shown in Fig.5.11, 5.12 and 5.13.

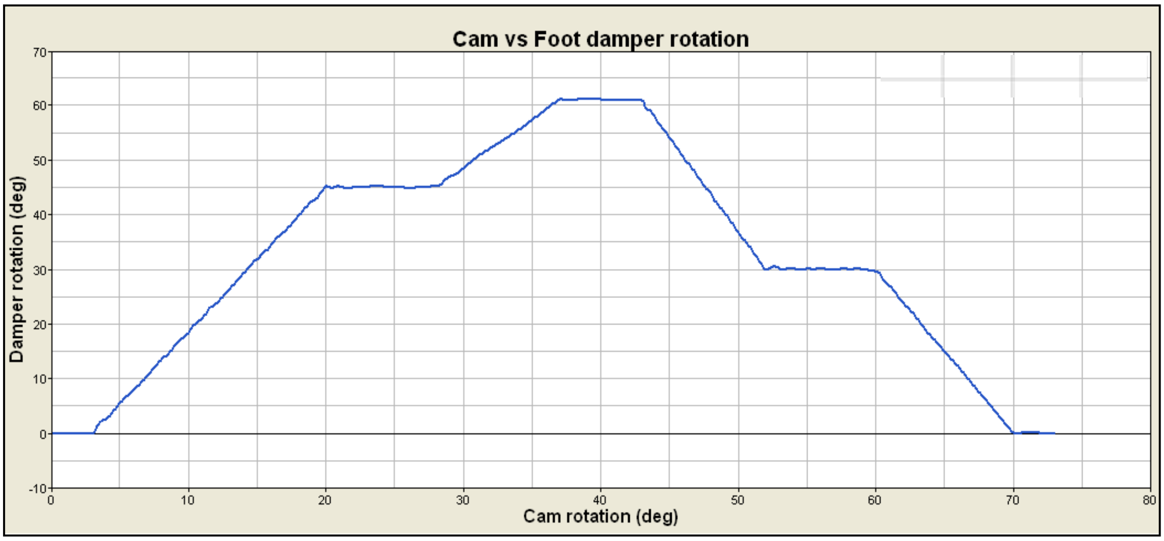

Figure 5.11: Cam vs. Foot damper rotation

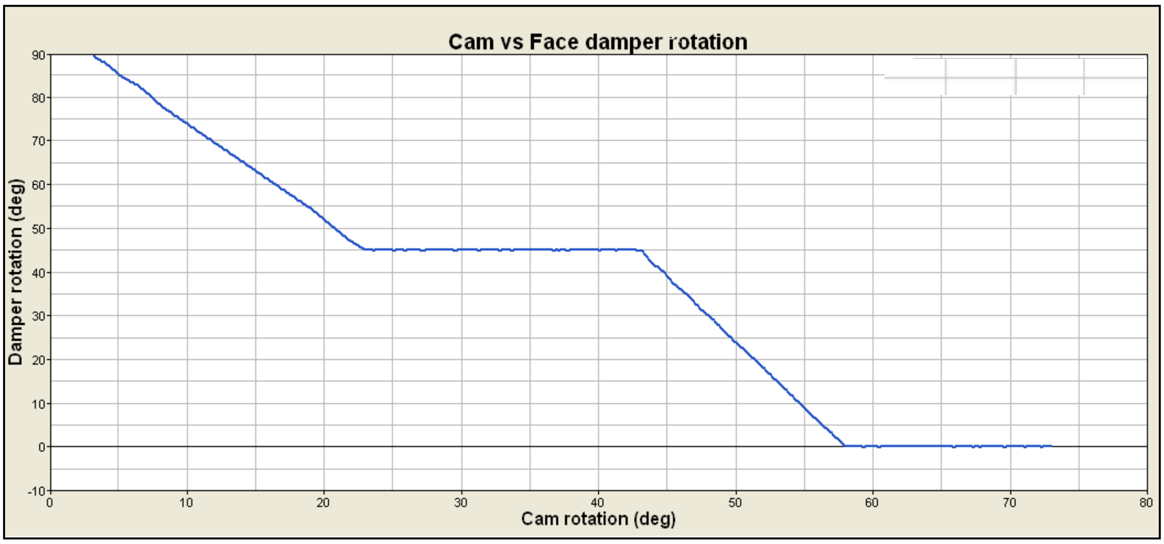

Figure 5.12: Cam vs. Face damper rotation

Displacement curves are obtained for the 73° rotation of the cam. The cam slots are made smoother, *i.e.*, without any sharp edges so that there is no obstruction to the movement of the pins inside those slots. After a few iterations, displacement graphs of the mechanism shown in Fig.5.11 and 5.12 have been reached.

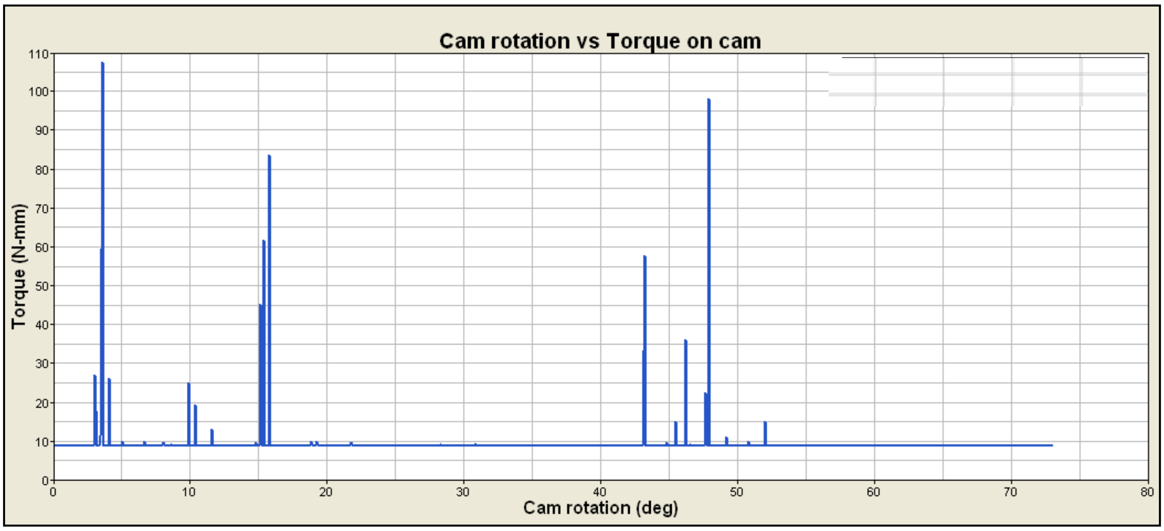

Figure 5.13: Cam rotation vs. Torque on cam

The average torque required to operate the cam is 9 $N-mm$. Spikes in the torque graph, Fig.5.13, are more and higher than are in the three link configuration mechanism. It can be seen from the Fig.5.8 and 5.13, that the value of torque required to operate the cam is lesser in 3 link mechanism design.

CHAPTER 6

CONCLUSION AND SCOPE FOR FUTURE WORK

6.1 CONCLUSION

An existing design of HVAC kinematic mechanism is studied and kinematically analysed. The results obtained revealed the information about the relative motion and design of mechanism components. A new method for cam design has been developed which is faster and simpler than the existing method. For the given problem two HVAC kinematic mechanism are designed, one with single link configuration and other with two link configuration. The assumptions include a constant angular velocity of the cam, and the rigidity of the parts in the mechanism. Using the same simulation methodology, kinematic analysis has been done for the two models and their results are compared. It is found that the single lever configuration used in the design led to higher torque requirement along with more space requirement. Torque required in the two link configuration is lesser than in the existing design, thus lowering the effort required to rotate the cam from the control panel.

With the use of the above approach, (1) a proper design of kinematics of linkages/damper movement has been arrived with acceptable forces applied for various damper movements; (2) a significant cost saving as the required number of physical prototypes reduced.

Thus, the use of CAE tools leads to an easy visualization and comparison of data thereby helping in the detection of problems early in the design cycle, reduced number of physical prototypes, resulting in significant saving of time and cost and last but not the least, more design iterations by incorporating simulation techniques.

6.2 SCOPE FOR FUTURE WORK

The present work can be further extended using the following:

a) Friction between the cam slots and pins can be considered in the analysis.
b) A cable (steel wire) connects the control knob on the dashboard of the car to the cam. When the knob is rotated, the wire pushes/pulls the cable pin present on the cam, thus rotating the cam clockwise/anticlockwise. The effect of this wire can be considered for further work.

c) The air pressure on the dampers can be taken into account and the results studied.

d) The discussed methodology can be extended to the simulation of other automobile mechanisms like wiper mechanism etc.

REFERENCES

[1] Alis A., Majid M.M.A, (2008), "Multibody dynamic analysis and topology optimization of Wiper Mechanism using Motionview / Motionsolve", *Proceeding of the HTC 2008, India.*

[2] Bertorelli N., Gugliotta A., Montanini R., Vadori R., (1998), "Structural crash analysis with ADAMS: a comparision between multibody and FEM approaches", *Proceeding of the12th European ADAMS Users' Conference, Paris,Nov.18th-19th* .

[3] Bauchau O.A., Ju C., (2006), "Modeling friction phenomena in flexible multibody dynamics", *Comput. Methods Appl. Mech. Engg.*, vol. 195, pp. 6909–6924.

[4] Popescu B., Hodges D.H., (2000), "On asymptotically correct Timoshenko-like anisotropic beam theory", *Int. J. Solids Struct.*, vol. 37, pp. 535–558.

[5] Canudas de Wit C., Olsson H., Astrom K.J., Lischinsky P., (1995)," A new model for control of systems with friction", *IEEE Trans. Automat. Control*, vol. 40, pp. 419–425.

[6] Espadafor F.J., Villanueva J.B., Garcia M.T., (2009), "Analysis of a diesel generator crankshaft failure", *Engineering Failure Analysis*, vol. 16, pp. 2333–2341.

[7] Flores P., Ambrosio J., (2004), "Revolute joints with clearance in multibody systems", *Computers and Structures,* vol. 82, pp. 1359–1369.

[8] Flores P., (2009), "Modeling and simulation of wear in revolute clearance Joints in multibody systems", *Mechanism and Machine Theory*, vol. 44, pp. 1211–1222.

[9] Greco M., Coda H.B., (2006), "Positional FEM formulation for flexible multi-body dynamic analysis", *Journal of Sound and Vibration*, vol. 290, pp.1141–1174.

[10] He B., Wang S., Gao F., (2010), "Failure analysis of an automobile damper spring tower", *Engineering Failure Analysis,* vol. 17, pp. 498–505.

[11] Khurmi R. S., Gupta J. K., (2002), "Theory of Machines", *S. Chand & Company Ltd., New Delhi.*

[12] Lankarani H.M., Nikravesh P.E., (1990), "A contact force model with hysteresis damping for impact analysis of multibody systems", J *Mech Des*, vol. 112, pp. 369-376.

[13] Mukras S., Kim N.H., Mauntler N.A., Schmitz T.L., Sawyer W.G., (2010), "Analysis of planar multibody systems with revolute joint wear", *Wear,* vol. 268, pp. 643–652.

[14] Magheri S., Malvezzi M., Meli E., Rindi A., (2011), "An innovative wheel–rail contact model for multibody applications", *Wear,* vol.271, pp. 462-471.

[15] Neto M.A., Ambrosio J.A.C., Leal R.P., (2006), "Composite materials in flexible multibody systems", *Comput. Methods Appl. Mech. Engg.*, vol. 195, pp. 6860–6873.

[16] Parvir E. Nikravesh, Gim G. ,(1990), "Ride and stability analysis of a sports car using multibody dynamic simulation", *Mathematical Computational Modelling,* vol. 14, pp. 953-958.

[17] Schirrmacher R., Bonneau A., (2003), "Dynamic Multibody Simulation of an Unit Injector System using ABAQUS/Explicit", *Proceeding of the 2003 ABAQUS Users Conference, Austria, Vienna, Nov. 24-25.*

[18] Sugiyama H., Shabana H.A., Mohamed A. O., Loh W., (2006), "Development of nonlinear elastic leaf spring model for multibody vehicle systems", *Comput. Methods Appl. Mech.Engg.,* vol 195, pp. 6925–6941.

[19] Teng T.L., Chang F.A., Liu Y.S., Peng C.P., (2008), "Analysis of dynamic response of vehicle occupant in frontal crash using multibody dynamics method", *Mathematical and Computer Modelling*, vol. 48, pp. 1724–1736.

[20] Vadhe R., Dave V., (2008), "Multi-Body simulation of Earthmoving Equipment using MotionView / MotionSolve", *Proceeding of the HTC 2008, India.*

[21] Xingguo M., Xiaomei Y., Bangchun W., (2007), "Multi-body Dynamics Simulation on Flexible Crankshaft System", *Proceeding of the 12th IFToMM World Congress, Besancon, France, June 18th-21th.*

[22] Yoo W.S., Kim M.S., Mun S.H., Sohn J.H., (2006), "Large displacement of beam with base motion:Flexible multibody simulations and experiments", *Comput. Methods Appl. Mech. Engg*., vol. 195, pp. 7036–7051.